NUS
National University
of Singapore

AN IMPROVED CODE RATE SEARCH SCHEME FOR ADAPTIVE MULTICODE CDMA

BY

CAI YINGHE (B.ENG)

A THESIS SUBMITTED

FOR THE DEGREEE OF MASTER OF ENGINEERING

DEPARTMENT OF ELECTRICAL AND COMPUTER

ENGINEERING

NATIONAL UNIVERSITY OF SINGAPORE

2003

Acknowledgments

First and foremost, I am grateful to my supervisors, Prof. Lawrence Wong and Prof. Paul Ho for their helpfulness and thoughtfulness and patience throughout my career here at NUS. It has been a great pleasure to have them as my supervisors.

I would also like to thank my friends who have been supporting and helping me during my study and work. I have been always benefited from their understanding and encouragement.

I would additionally like to thank NUS for giving me the opportunity to pursue my Master degree in Singapore and providing the wonderful studying and working environments.

Last but not least, I would like to thank my family whose love motivates me to achieve the best of myself in life.

Table of Contents

List of Figures

List of Tables

Abbreviations

AGC	Automatic Gain Control
AWGN	Additive White Gaussian Noise
BER	Bit Error Rate
BPSK	Binary Phase Shift Keying
CDMA	Code Division Multiple Access
CLPC	Close Loop Power Control
FDMA	Frequency Division Multiple Access
FFT	Fast Fourier Transformation
IFFT	Inverse Fast Fourier Transformation
MAI	Multiple Access Interference
pdf	Probability Density Function
PN	Pseudo-Noise
QAM	Quadrature Amplitude Modulation
QoS	Quality of Service
SIR	Signal to Interference Ratio
TDMA	Time Division Multiple Access
TPC	Truncated Power Control
WSS	Wide-Sense Stationary

Summary

Transmission over Rayleigh fading mobile radio channel are subjected to error bursts due to deep fades. This can be ameliorated through the use of power control whereby the transmitted rate is unchanged. However, this both increases transmitted power requirements and the level of cochannel interference. Hence a lot of works are motivated to the notion of joint rate and power adaptation. In [19] several combined rate and power adaptation schemes are proposed to maximize the uplink throughput in adaptive multicode CDMA system under different scenarios. One of the schemes is to search the optimal rate vector from a table including all achievable vectors when the codes are limited to be a finite integer. The problem is that the size of the search table would be very large, which makes the search scheme inefficient.

In this report, with the same system model as [19], we propose a scheme with the aim to reduce the search complexity. Firstly, we apply appropriate boundary conditions to narrow down the searching complexity. All these boundary conditions are given with strict proofs. Next we set the initial rate vector according to the boundary conditions. Adaptively, we adjust the rate vector from initial state to its optimal state. We observe that the search complexity is greatly reduced using simulations. Before that, we build a Rayleigh fading channel simulator based on Clarke's scattering model. This simulator is used to provide the necessary channel information for simulation of the improved scheme.

Chapter 1 Introduction

1.1 Mobile Radio Channel

Radio waves propagate from a transmitting antenna, and travel though free space undergoing absorption, reflection, refraction, diffraction, and scattering. They are greatly affected by the ground terrain, the atmosphere, and the objects in their path, like buildings, bridges, hills, trees, etc. These physical phenomena are responsible for most of the characteristic features of the received signal.

In most of the mobile or cellular systems, the height of the mobile antenna may be smaller than the surrounding buildings. Therefore, the existence of a direct or line-of-sight path between the transmitter and receiver is highly unlikely. In such a case, propagation is mainly due to reflection and scattering from the buildings and by diffraction over them. So, in practice, the transmitted signal arrives at the receiver via several paths with different time delays creating a multipath situation as shown in Figure1.1.

At the receiver, these multipath waves with randomly distributed amplitudes and phases combine to give a resultant signal that fluctuates in time and space. Therefore, a receiver at one location may have a signal that is much different from the signal at another location, only a short distance away, because of the change in the phase relationship among the incoming radio waves. This causes significant fluctuations in the signal

amplitude. This phenomenon of random fluctuations in the received signal level is termed as *fading*.
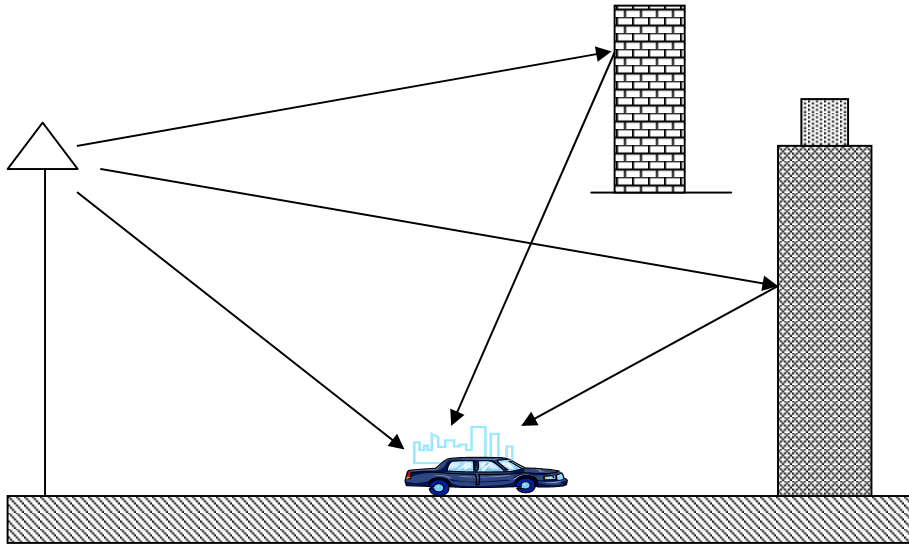
Figure 1.1   Mechanism of Radio Propagation in a Mobile Environment

The short-term fluctuation in the signal amplitude caused by the local multipath is called small-scale fading. It is observed over distances of about half a wavelength. On the other hand, long-term variation in the mean signal level is called large-scale fading. The latter effect is a result of movement over distances large enough to cause gross variations in the overall path between the transmitter and the receiver. Large-scale fading is also known as *shadowing*, because these variations in the mean signal level are caused by the mobile unit moving into the shadow of surrounding objects like buildings and hills. Due to the effect of multipath, a moving receiver can experience several fades in a very short duration, or in a more serious case, the vehicle may stop at a location where the signal is in deep fade. In such a situation, maintaining good communication becomes an issue of great concern.

1.2 CDMA System

The radio frequency spectrum has long been viewed as a vital natural resource. Protecting and enhancing this limited resource has become a very important activity since the radio frequency spectrum is primarily a finite resource, although technological advances continue to expand the range of usable frequencies. In the past few decades, some multiple access strategies have been employed to be used for terrestrial cellular mobile radio systems such as FDMA, TDMA and CDMA. Comparing to FDMA and TDMA, CDMA provides the following advantages:

- Multipath fading mitigation---wideband spread-spectrum signals are suitable for diversity combining reception;

- Interference rejection---unlike narrowband signals, spread-spectrum signals are less sensitive to narrowband interference;

- Graceful performance degradation---the capacity of CDMA is a soft limit, i.e., more user can be accommodated at a cost of the BER; on the other hand, FDMA or TDMA has a hard capacity limit where extra users will be denied service;

- Privacy and protection against eavesdropping.

In response to an ever-accelerating worldwide demand for mobile and personal portal communications, based on spread-spectrum technology, CDMA has been widely deployed in cellular system.

In direct-sequence spread-spectrum, a baseband data signal is spread to wideband by pseudo-noise (PN) or a spreading code. The spread-spectrum signal has a low power spectral density. It appears almost like background noise to a casual receiver and normally

causes little interference. When two spread-spectrum signals are sharing the same frequency band, there is a certain amount of crosstalk, or mutual interference. However, unlike in narrowband transmissions, the interference is not disastrous. This is because the spreading codes is designed with low crosscorrelation values so that they are nearly orthogonal, i.e., the crosscorrelation function is almost zero. As a result, many spread-spectrum signals share the same frequency channel and there is no severe mutual interference. In this scenario, the system performance degrades gracefully with increasing number of users.

1.3 Power Control Model in CDMA System

Power control is a valuable asset in any two-way communications system. It is particularly important in a multiple access terrestrial system where users' propagation loss can vary over many tens of decibels. In a CDMA system, the power at the cellular base station received from each user over the reverse link must be made nearly equal to that of all others in order to maximize the total user capacity of the system. Very large disparities are caused mostly by widely differing distances from the base station and, to a lesser extent, by shadowing effects of the buildings and other objects. Such disparities can be adjusted individually by each mobile subscriber unit simply by controlling the transmitted power according to the automatic gain control (AGC) measurement of the forward link power received by the mobile receiver. Generally, this is not effective enough: the forward and reverse link propagation losses are not symmetric, particularly when their center frequencies are widely separated from one another. Thus, even after adjustment using

"open loop" power control based on AGC, the reverse link transmitted power may differ

by several decibels from one subscriber to the next.
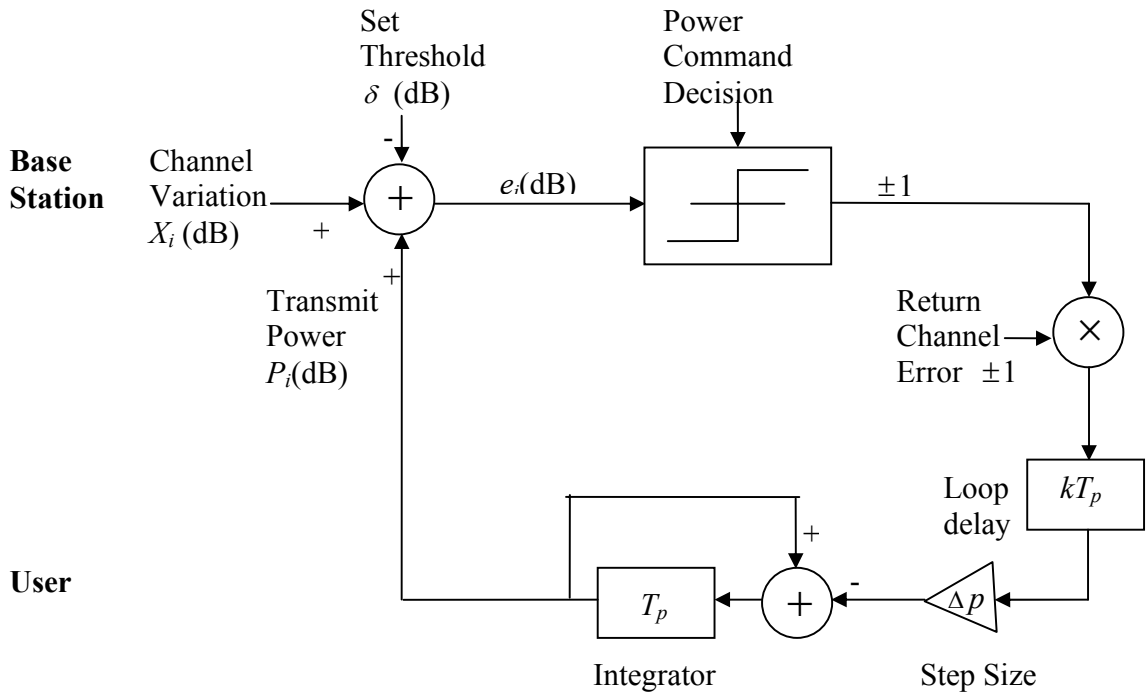
Figure 1.2   Closed loop Feedback Power Control Model

The remedy is "closed loop" power control. Closed loop power control (CLPC)   refers to

a situation where the base station, upon determining that any mobile's received signal on

the reverse link has too high or too low a power level (or more precisely the signal-to-

interference level), a 1-bit command is being sent by the base station to the mobile over

the forward link to command the mobile to lower or raise its relative power by a value of

ΔdB. Delay occurs in time required to send the command and execute the change in the

mobile's transmitter. A CLPC feedback power control model is shown in Figure 1.2. The

user transmitting signal power S_i (dB) is updated by a fixed step Δp (dB) every T_p

seconds, where T_p is the power control sampling period , subscript i indicates the ith sampling interval, and " δ dB" denotes the dB value of a quantity δ . A lag of k sampling intervals accounts for possible additional loop delay in a real implementation. The error e_i (dB) is the difference between the received SIR $p_i x_i$ (dB) and the set SIR threshold δ (dB), where x_i includes the effects of the time-varying channel attenuation and uplink interference.

1.4 Multirate Technologies in CDMA System

The existing mobile communication systems mainly support speech services. Also in future systems speech is expected to be the main service, but with higher quality than in the systems of today, and maybe in conjunction with video. Other expected services are image transmission with high resolution and color and moving pictures, e.g. video transmission. Further, the increasing demand for information in our society requires an easy way to access and process information. Therefore data transmission and wireless computing are necessary services in any future system. If we translate this to transmission of bits, we require rates from about 10kbps to 1Mbps, with bit error rates from around 10^{-2} for speech and images to 10^{-6} or lower for data transmission. There are serveral ways to design a multi-rate system. In [3], several schemes have been investigated and comparisons have been made to compare their performances in terms of BER.

1.4.1 Multi-Modulation Scheme

Usually BPSK is used as modulation in a DS/CDMA system. In spite of this, we can define a multi-modulation system with n rates $R_1 > R_2 > .... > R_n$, as a system where all users

have the same symbol rate and processing-gain $N = B/R_n$. Here B is the system

bandwidth and R_n is the bit rate for BPSK users. The bit error probability of user k in an

M-ary square lattice QAM-subsystem i is [3]

$$P_b = \frac{4}{\log(M)} \frac{\left(\sqrt{M}-1\right)}{\sqrt{M}} Q\left(\left[\frac{M-1}{3}\left(\frac{N_0}{\log(M)E_b} + \frac{2}{3N}\left(\sum_{j=1}^{n} \frac{R_j}{R_i} K_j - 1\right)\right)\right]^{-1/2}\right) \qquad (1.1)$$

where E_b/N_0 refers to the required signal-to-noise ratio per bit, R_j is the bit rate of

subsystem j, K_j is the number of users in the jth subsystem, $\log(\bullet)$ is the logarithm of

base 2 and $Q(\bullet)$ is the complementary error functoin . The modulation level, that is, the

number of symbols in the signal space, is controlled by the bit rate and given

by $M = 2^{(R_i/R_n)}$.

1.4.2 Multi-Channel or Multi-Code Scheme

With the multi-code transmission scheme, a high-rate bit rate stream is first split into

several fixed low-rate bit rate streams. The multiple data streams are spread by different

short codes with the same chip rate and are added together. Multiple codes for a high-rate

call should be orthogonal over an information bit interval to reduce the intercode

interference. A random scrambling long pseudonoise (PN) code common to all parallel

short code channels can be applied after spreading. The long PN code does not affect any

orthogonality property between the parallel channels but makes the transmission

performance independent of the time-shifted auto- and cross-correlation properties of the

spreading codes, which is one of the distinguishing features of concatenated orthogonal

PN spreading sequences. Suppose the bit error performance for a multi-channel system with constant processing-gain N, chip period T_c and QPSK modulation is given by [3]

$$P_b = Q\left(\left[\frac{N_o}{2E_b} + \frac{2}{3N}\left(\sum_{i=1}^{n}\frac{R_i}{R_o}K_i - 1\right)\right]^{-1/2}\right) \qquad (1.2)$$

where R_0 is the bit rate for a single QPSK channel and the other parameters have the same definition as in (1.1).

1.4.3 Multi Processing-Gain Scheme

The most natural way, or at least the most conventional way, to achieve multi-rate is to vary the processing gain, and accordingly spread all users independently of their bit rates to the same bandwidth B. Consider a multi processing-gain system with all users using BPSK modulation and a constant chip period T_c. The bit rates supported by the system are ordered as $R_1=1/T_1>R_2=1/T_2>....>R_n=1/T_n$ with the processing-gains $N_i=B/R_i$. The performance of user with rate R_k in BPSK modulated system may be expressed as [3]

$$P_b = Q\left(\left[\frac{N_o}{2E_b} + \frac{1}{3N_i}\left(\sum_{j=1}^{n}\frac{R_j}{R_i}K_j - 1\right)\right]^{-1/2}\right). \qquad (1.3)$$

1.4.4 Comparison of The Above Schemes

Besides those multi-rate schemes mentioned above, there exist other schemes such as *Multi Chip-Rate Systems* [6] and *Miscellaneous Multi-Rate Schemes* [7]. In [3], the author has investigated these schemes followed by some useful conclusions. Firstly, it is possible to use multi-modulation scheme, which only degrades the performance for the users with high data rates, that is, users that use higher modulation than QPSK. Secondly, a multi

processing-gain scheme has almost the same performance as a multi-code scheme. However, if the system is to support many data rates up to about 1Mbps, a multi processing-gain system will only have a small processing gain for the highest rates and is therefore sensitive to external interference.   Further, a considerable amount of inter-symbol interference will be present. The multi-code scheme has the same processing gain for all users, independent of their data rates. It may also be easier to design codes that have good properties and construct a multi-user receiver if only on processing gain is used in the system. One disadvantage of the multi-channel is the need for mobile terminals with a linear amplifier for users with high rates, because the sum of many channels gives rise to large amplitude variations. The comparison of these two schemes is presented in [10].

1.5 Joint Power and Rate Adaptation in DS-CDMA System

Multirate DS-CDMA and adaptive modulation form the foundations for the third generation of wireless communication systems, and there is previous work in this area. However, adaptive CDMA remains a relatively unexplored area of research. "Adaptation" in the context of CDMA systems has been mostly synonymous with power control. The need to support multiple rates and the emergence of various multirate CDMA schemes using multiple codes, multiple processing gains, and multirate modulations have shifted the focus from power adaptation alone to joint power and rate adaptation.

The basic principle of joint power and rate adaptation is to send more information during good channel conditions. As the channel condition worsen, lower information rate are applied in order to maintain adequate transmission quality. Wasserman and Oh [11]

considered optimal (throughput maximizing) dynamic spreading gain control with perfect power control. Adaptive code rates were considered in [14]. Hashem and Sousa [12] showed that limiting the increase in power to compensate for mulitpath fading, and getting the extra gain required by reducing the transmission rate, can increase the total throughput by about 231% for flat Rayleigh fading. Kim and Lee [13] showed the power gains achieved by the same scheme, and also considered truncated rate adaptations. In [19], Jafar and Goldsmith consider an optimal adaptive rate and power control strategies to maximize the total average throughput in a multicode CDMA system, subject to an instantaneous BER constraint.

1.6 Contributions

Due to the fact that a search scheme presented in [19] is inefficient in terms of search complexity when the code rate is restricted to be a discrete integer, we develop an improved scheme to reduce the search complexity without sacrificing system performance. The contributions, which are elaborated throughout this thesis, are listed as follows:

- We build up an effective multipath channel model with Rayleigh distribution. The simulated results are tested with first-order and second-order statistical analysis.

- We can narrow down the search range by applying proper boundary conditions. These boundary conditions are given with strict proofs. It enables us to analyze the case where full quota of code rate M is an unlimited integer.

- When it comes to searching the optimal rate, we can firstly set the initial rate state within the boundaries. Next, we adaptively adjust the initial rate to the optimal one. By doing so, the search complexity can be greatly reduced.

- We perform simulations to examine the performances of two search scheme. The results of the simulations justify our claim about the search complexity saving.

- We also consider the cases where full rate quota M takes limited values from 5 to 15. With the improved scheme, the search complexities are found to be reduced significantly too. Moreover, we find that the larger full quota M is, the better the improvement we can receive.

1.7 Report Layout

Chapter 1 of this report has provided a concise coverage of the relevant materials that are required for the understanding of the subject matter of this dissertation. In Chapter 2, a flat Rayleigh fading channel simulation model is described and the simulated results are compared with the theoretical values. Next, in Chapter 3, we proposed an improved rate search scheme in multicode CDMA system. The algorithm will be described in detail. Lastly we conclude the report with a summary in Chapter 4. All source codes are available in Appendix A and B

Chapter 2 Statistical Modeling of Flat Rayleigh Fading

Mobile radio communications in an urban environment actually takes place over a fading channel. In the fading channel, a signal from the transmitter arrives at the receiver via many paths, due to reflections and refractions from the surrounding buildings and the terrain. As the signal waves travel through the environment, they are reflected and their phases are then altered randomly. In this chapter, a computer simulation with MATLAB of flat Rayleigh fading channel is described. This simulation should be of interest to all those who studies involve parameters of a mobile system that interact strongly with the radio environment.

2.1 Scattering Model for Flat Fading

Several multipath models have been suggested to explain the observed statistical nature of the mobile channel. Among them, Clarke's model [4] is based on scattering and is widely used for modeling wireless environment in urban area where the direct path is almost always blocked by the buildings and other obstacles.

Clarke developed a model where the statistical characteristics of the electromagnetic fields of the received signal at the mobile are deduced from scattering. The model assumes a fixed transmitter with a vertically polarized antenna, the field incident on the mobile antenna is assumed to be comprised of many azimuthal plane waves with arbitrary carrier phases, arbitrary azimuthal angles of arrival, and each wave having equal average amplitude. The equal average amplitude assumption is based on the fact that in the

absence of a direct line-of-sight path, the scattered components arriving at a receiver will experience similar attenuation over small-scale distances.

Figure 2.1 shows a diagram of a plane ray incident on a mobile traveling at a velocity v, in the x-direction. The angle of arrival is measured in the x-y plane with respect to the direction of motion. Every wave that is incident on the mobile undergoes a *Doppler shift* due to the motion of the receiver and arrives at the receiver at the same time. For the nth wave arriving at angle to x-axis, the *Doppler shift* in Hertz is given by

$$f_n = \frac{v}{\lambda} \cos \alpha_n \qquad\qquad (2.1)$$

where λ is the wavelength of the incident wave.
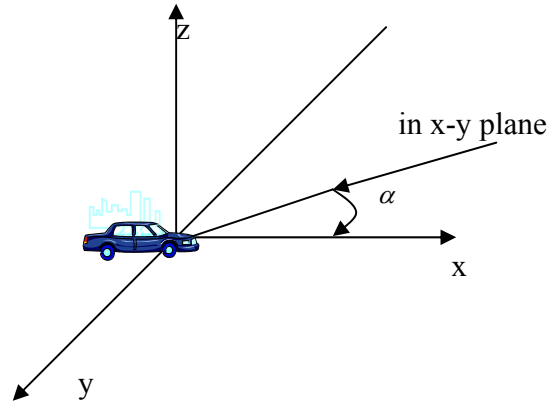
Figure 2.1   Fading Scenario

N independent incident rays arriving at the mobile receiver with different phases, amplitudes and angles of arrival combine together to produce a multipath signal of the following form:

$$S(t) = \sum_{i=1}^{N} \left[A_i \cos\left(w_c t + 2\pi f_D \cos\alpha_i t + \Phi_i\right)\right] \tag{2.2}$$

where

$$f_C \quad = \text{carrier frequency}$$

$$w_c = \text{angular carrier frequency}$$

$$\Phi_i = \text{phase of the } i^{th} \text{ incident ray}$$

$$\alpha_i = \text{angel of arrival of the } i^{th} \text{ incident ray}$$

$$f_D = \text{maximum Doppler frequency shift}$$

$$A_i = \text{amplitude of the } i^{th} \text{ incident ray}$$

$$\lambda = \text{carrier wavelength}$$

Consequently, the transmission of an unmodulated carrier is received as a multipath signal, whose spectrum is not a single carrier frequency, but contains frequencies up to $f_C \pm f_D$.
Using algebraic manipulation,

$$S(t) = \sum_{i=1}^{N} \left[A_i \cos(w_C t)\cos(2\pi f_D \cos\alpha_i t + \Phi_i) + A_i \sin(w_C t)\sin(2\pi f_D \cos\alpha_i t + \Phi_i)\right]$$
$$= x(t)\cos(w_C t) - y(t)\sin(w_C t) \tag{2.3}$$

where

$$x(t) = \sum_{i=1}^{N} \left[A_i \cos(2\pi f_D \cos\alpha_i t + \Phi_i)\right]$$

and $\quad y(t) = \sum_{i=1}^{N} \left[A_i \cos(2\pi f_D \cos\alpha_i t + \Phi_i)\right]$.

The received multipath signal is written in the form of a random process which is centered at some frequency f_C. $x(t)$ and $y(t)$ are the inphase and the quadrature phase components of $s(t)$ respectively and are both random process. However, the Central Limit Theorem says that the sum of a large number of independent random variables result in a Gaussian distribution. Hence, if N is large enough, $x(t)$ and $y(t)$ can be characterized as two independent Gaussian random processes with zero means and common variance σ^2.

The expression for the multipath signal can be rewritten in terms of its envelope and phase components:

$$S(t) = \mathrm{Re}\left[T(t)e^{jwt} \right] = \mathrm{Re}\left[re^{j(w_C+\alpha)} \right] = r(t)\cos(w_C t + \Phi(t)) \tag{2.4}$$

where

$$T(t) = x(t) + jy(t) = \sqrt{x(t)^2 + y(t)^2}\, e^{j\tan^{-1}\left(\frac{y(t)}{x(t)}\right)} = r(t)e^{j\Phi(t)}$$

$$r(t) = \sqrt{x(t)^2 + y(t)^2}$$

and
$$\Phi(t) = \tan^{-1}\left(\frac{y(t)}{x(t)} \right)$$

in which the *probability density function* (pdf) , $P(r)$ of $r(t)$ is

$$P(r) = \left(\frac{r}{\sigma^2} \right)\exp\left(\frac{-r^2}{2\sigma^2} \right) \qquad ,$$

(2.5)

and the pdf $P(\Phi)$ of $\Phi(t)$ is

$$P(\Phi) = \frac{1}{2\pi} \quad , \quad 0 \le \Phi(t) \le 2\pi. \tag{2.6}$$

2.2 Simulation Model of Flat Fading Channel

It is often useful to simulate multipath fading channels in hardware or software. A popular simulation method uses the concept of in-phase and quadrature modulation paths to produce a simulated signal with spectral and temporal characteristics close to practical measured data.

As shown in Figure 2.2, two independent Gaussian noise sources are used to produce in-phase and quadrature fading branches. After the Doppler filters, each branch of the original Gaussian random processes is transformed into another Gaussian random process with its power spectrum reshaped. Great concern is given to how the Doppler filter works and how it is implemented.
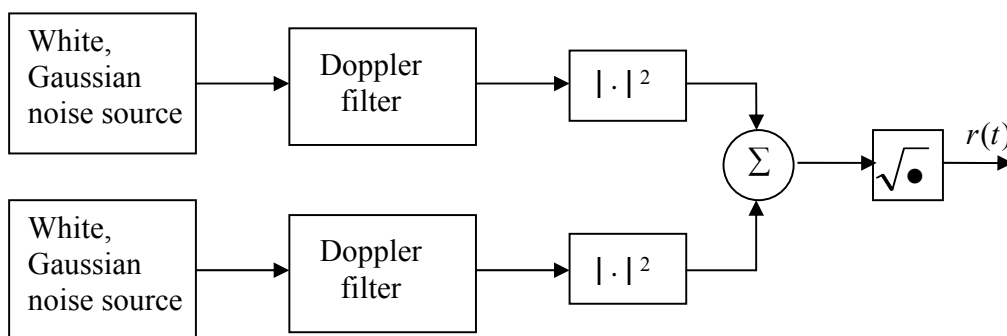
Figure 2.2   Flat Rayleigh Fading Channel Model Block Diagram

2.2.1 White Gaussian Noise Source

Each of the two independent whit Gaussian noise sources produces a white Gaussian sequence having zero mean and unit variance.

2.2.2 Doppler Filter

The Doppler filter is actually a spectral filter. It converts the power spectrum of the input white Gaussian noise into another Gaussian process having the same mean but different power spectrum and variance. As a result , the spectrum of the filter's output is the desired power spectral density, which in this case is of the form in Figure 2.3   [2].

$$S(f) = \left(\frac{\sigma^2}{\pi \sqrt{f_D^2 - f^2}} \right) \qquad (2.7)$$
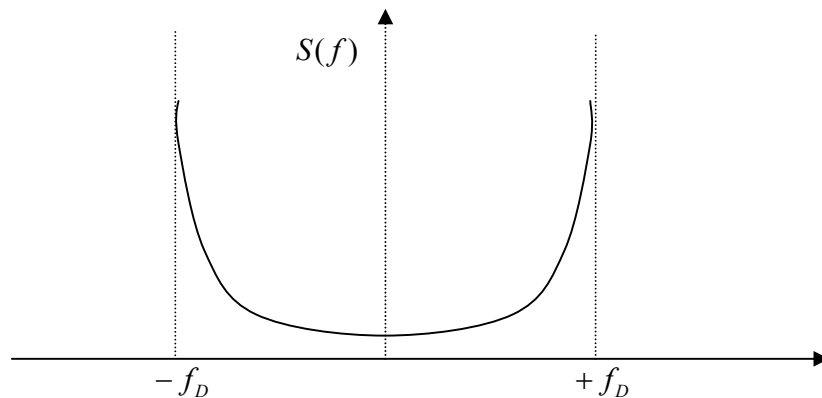
Figure 2.3   Power Spectrum of the Flat Rayleigh Faded Signal

$S(f)$ is common power spectral density of $x(t)$ and $y(t)$. Each of the multipath components has its own carrier frequency which is slightly different from the transmitted carrier frequency.

Figure 2.4 shows a simplified diagram of the operation of the Doppler filter.
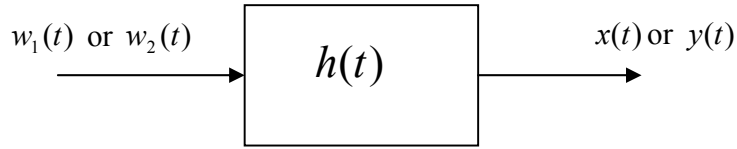
Figure 2.4   Doppler filter

Here,

$h(t)$ = Doppler filter's impulse response

$w_1(t)$, $w_2(t)$= white Gaussian noise process having zero mean and unit variance

$x(t)$ = Output sequence of the first Doppler filter

$y(t)$ = Output sequence of the second Doppler filter

In the continuous time domain,

$$x(t) = \int_{-\infty}^{\infty} \left[h(k)w_1(t-k) \right] dk \tag{2.8}$$

$$y(t) = \int_{-\infty}^{\infty} \left[h(k)w_2(t-k) \right] dk \tag{2.9}$$

In the discrete time domain,

$$x(m) = \sum_{k=-\infty}^{k=\infty} \left(h[m]w_1[m-k] \right) \tag{2.10}$$

$$y(m) = \sum_{k=-\infty}^{k=\infty} \left(h[m]w_2[m-k] \right) \tag{2.11}$$

The following describe determination of the Doppler filter's impulse response $h(t)$.

$$S(f) = \left| H(f) \right|^2 S_w(f) \tag{2.12}$$

$$\left(\frac{\sigma^2}{\pi\sqrt{f_D^{\,2} - f^2}} \right) = |H(f)|^2 \left(\frac{N_O}{2} \right) \tag{2.13}$$

The amplitude component of frequency response of the Doppler filter can be expressed as follows.

$$H(f) = \sqrt{\frac{2}{N_O}} \left(\frac{\sigma^2}{\pi\sqrt{f_D^{\,2} - f^2}} \right)^{\frac{1}{2}} \tag{2.14}$$

Performing *Inverse Fourier Transform* (IFT) on the frequency domain signal, we have

$$
\begin{aligned}
h(t) &= \int_{-\infty}^{\infty} H(f) e^{j2\pi ft} df \\
&= \int_{-f_D}^{f_D} \left(\sqrt{\frac{2\sigma^2}{N_O \pi}} \right) \left(\sqrt{\frac{1}{\sqrt{f_D^{\,2} - f^2}}} \right) e^{j2\pi ft} df \\
&= \varepsilon \int_{-f_D}^{f_D} \left(\sqrt{\frac{1}{\sqrt{f_D^{\,2} - f^2}}} \right) e^{j2\pi ft} df
\end{aligned}
\tag{2.15}
$$

where

$$\varepsilon = \left(\sqrt{\frac{2\sigma^2}{N_O \pi}} \right)$$

There are two ways to compute the Doppler filter's impulse response. One way is to perform the above integration directly [12]. The resultant form is given as

$$h(t) = \sqrt{\frac{2\sigma^2 f_D}{N_O}} \left[\frac{\Gamma\left(\frac{3}{4} \right) J_{1/4}(2\pi f_D t)}{(\pi f_D t)^{1/4}} \right] \tag{2.16}$$

where $J(\bullet)$ is Bessel function and $\Gamma(\bullet)$ is Gamma function.

The other way is to convert $H(f)$ to its time domain by *Inverse Fast Fourier Transformation* (IFFT). Firstly, sample $H(f)$ to make it a discrete signal. Let $f = m\Delta f$ (Δf is the sampling frequency interval).

Then $H(f)$ can be rewritten as

$$
\begin{aligned}
H(m\Delta f) &= \sqrt{\frac{2}{N_O}} \left(\frac{\sigma^2}{\pi \sqrt{f_D^2 - (m\Delta f)^2}} \right)^{\frac{1}{2}} \\
&= \sqrt{\frac{2}{N_O}} \left(\frac{\sigma^2}{\pi \Delta f \sqrt{(f_D / \Delta f)^2 - m^2}} \right)^{\frac{1}{2}}
\end{aligned}
$$

(2.17)

Secondly, convert the discrete signal to its time domain by performing *IFFT* on $H(m\Delta f)$ with respect to m.

Lastly, take the real part of the result of the last step as the impulse response sequence. Namely,

$$
h(n) = \mathrm{Re}\{IFFT(H(m\Delta f))\}
$$

(2.18)

where Δf is the sampling frequency interval.

The typical full (double sided) impulse response $h(t)$ is shown in Figure 2.5.

From Figure 2.4, we can see that the implementation of Doppler filter is equivalent to performing discrete convolution between $w_1(t)$ and $h(t)$, which we can manipulate by

using the tool of *Fast Fourier Transform* (FFT) for computing simplicity. For the upper

branch of Figure 2.2 in the continuous domain,

$$x(t) = w_1(t) \otimes h(t)$$

$$= F^{-1}\left[F\left(w_1(t)\right) \times F(h(t)\right]$$

$$= F^{-1}\left[F\left(w_1(t)\right) \times H(f)\right]$$

where $\otimes$ represents convolution operation, $F(\bullet)$ denote *Fourier Transformation*   and

$F^{-1}(\bullet)$ is used to denote *Inverse Fourier Transformation* .
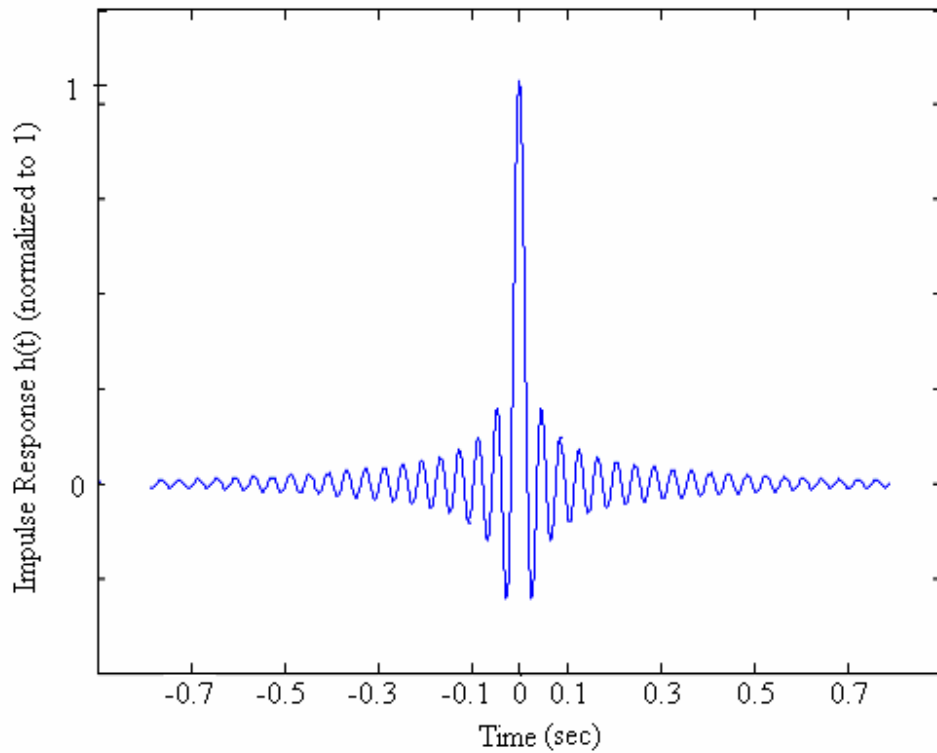
Figure 2.5   Typical Full Impulse Response of Doppler Filter (sample)

In discrete domain,

$$x(n) = IFFT\big[FFT\big(w_1(n)\big) \times H(n)\big] \qquad (2.19)$$

The lower branch can be manipulated in a similar way as follows.

In continuous domain,

$$y(t) = F^{-1}\big[F\big(w_2(t)\big) \times H(f)\big].$$

In discrete domain,

$$y(n) = IFFT\big[FFT\big(w_2(n)\big) \times H(n)\big].$$

To visualize the above procedure, the following figure shows the implementation of Doppler filter with its inner structure. The discretized form of white Gaussian noise process is fetched into Doppler filter chunk by chuck. If each chunk contains a length of L samples and the length of the Doppler filter's finite impulse response is D, then the length of the effective output block is at least $(L + D - 1)$ long. For the extra portion of $(D - 1)$, overlap operation is needed to add this extra portion to the next block.
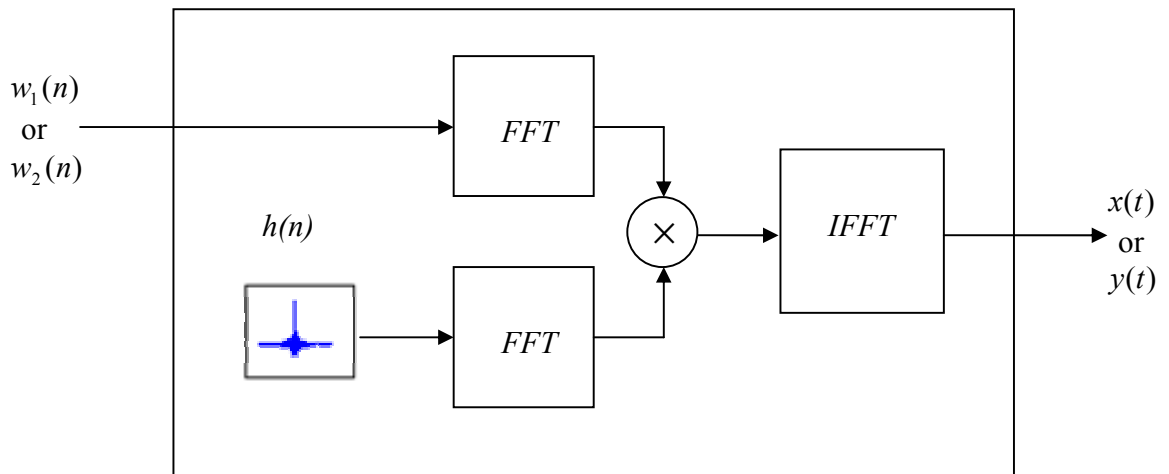
Figure 2.6   The Inner Structure of Doppler Filter

2.3 Implementation of Simulation

It is well known that MATLAB is a high-performance language for its powerful computational abilities. It features a vast collection of useful signal processing functions which make programming an easy and quick job. Hence, we choose MATLAB as the programming language for the simulation. The following diagram describes the flow of the important steps involved in simulator software.

```
┌─────────────────────┐
│ assume and set      │
│ the necessary       │
│ parameters for      │
│ the system          │
└─────────────────────┘
          ⇓
┌─────────────────────┐
│ generate the        │
│ white Gaussian      │
│ noise sequences     │
└─────────────────────┘
          ⇓
┌─────────────────────┐
│ generate the        │
│ Doppler filter's    │
│ impulse response    │
└─────────────────────┘
          ⇓
┌──────────────────────────────────────┐
│ carry out the discrete convolution   │
│ operations block by block, i.e. pass │
│ the white Gaussian sequences through │
│ the Doppler filters to shape their   │
│ spectrum                             │
└──────────────────────────────────────┘
          ⇓
┌──────────────────────────────────────┐
│ 1. obtain Rayleigh faded envelope    │
│ 2. obtain the pdf of the envelope    │
│    and compare with theoretical pdf  │
│ 3. obtain the autocorrelation of the │
│    envelope and compare with the     │
│    theoretical values                │
└──────────────────────────────────────┘
```

Figure 2.7   Simulator Software Block Schematic View

2.4 Verification of Simulation Results

2.4.1 Rayleigh Faded Envelope

The following figure is obtained from simulation showing the typical Rayleigh fading gain in dB. It can be observed that this channel fading gain varies dramatically as the vehicle moves. Sometimes the deep fade could be as low as -40dB which is very harmful to signals. As can be illustrated in the following chapter, one method to overcome this is to use both rate and power adaptation.
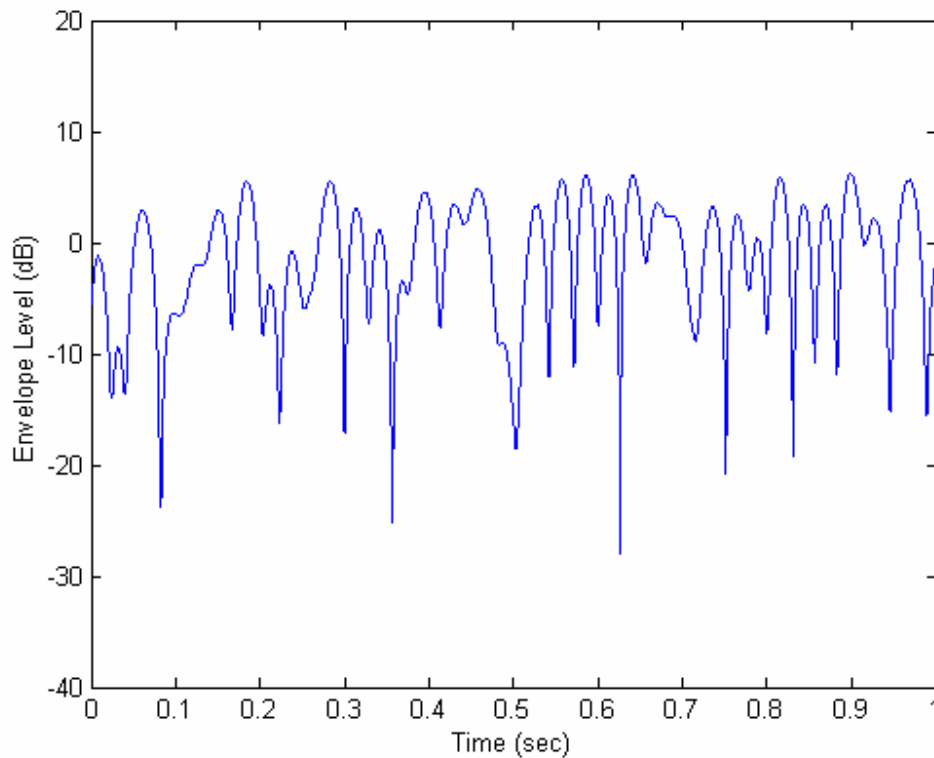
Figure 2.8   Typical Rayleigh Fading Envelope

From figure 2.7, we can write a program to simulate the envelope random process $r(t)$. Please refer to the source code included in Appendix A for more details. In order to verify

that the envelope is indeed Rayleigh-distributed and determine the degree of closeness between the simulated and theoretical values, statistical testing can subsequently be used to establish the validity of the fading simulation model.   To achieve a reasonable performance, it is recommended that the number of the sampling points should be more than 10^5. Both the first-order and second- order statistics are performed to test the results. The first-order statistics here refers to the distribution of amplitude envelope $r(t)$ and the second order statistics refers to the autocorrelation of $r(t)$.

The following set of parameters is used for the testing

- Carrier frequency =900MHz

- Maximum Doppler frequency shift = 20Hz

- Sampling rate / Maximum Doppler frequency shift=100

- Mean amplitude of *r(t)* is normalize to 1.0

- Number of simulation points = 122880

2.4.2 The First-Order Statistics (Distribution of *r(t)*)

The following figure shows the simulated distribution of $r(t)$ as well as its theoretical curve indicated by (2.21).   Since we have normalized the mean value of *r(t)* to unity, σ in (2.20) can be determined by applying the following relation

$$r_{mean} = E(r) = \int_0^\infty rp(r)dr = \sigma\sqrt{\frac{\pi}{2}} = 1.2533\sigma = 1, \tag{2.20}$$

where $p(r) = \dfrac{r}{\sigma^2}\exp(-\dfrac{r^2}{2\sigma^2})$. \hfill (2.21)
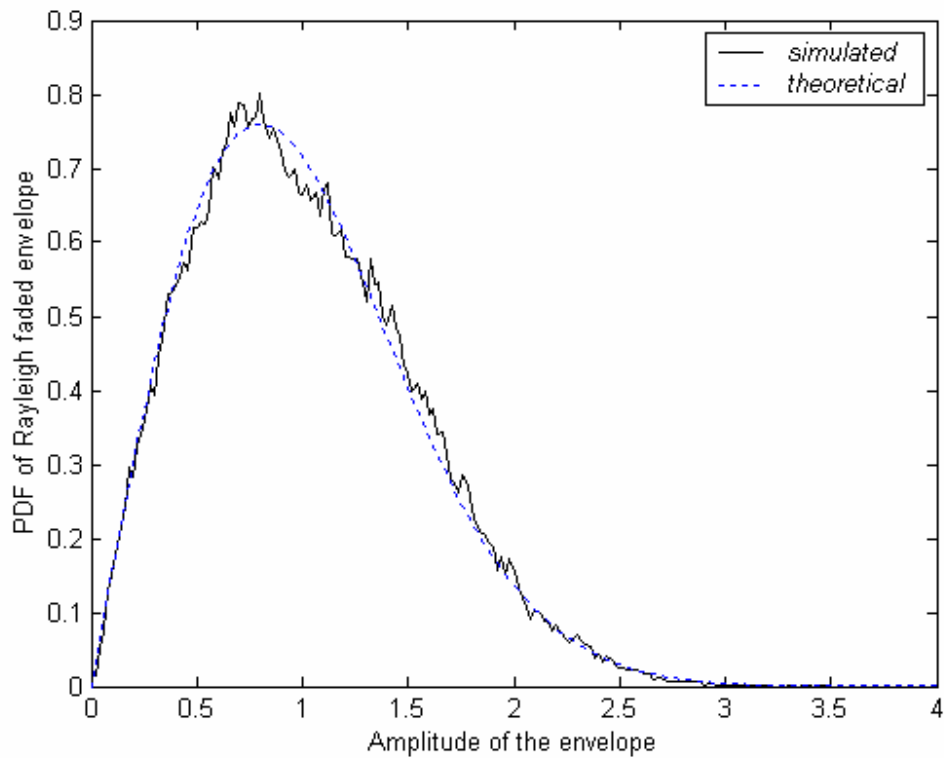
Figure 2.9   pdf of Rayleigh Faded Envelope

It can be observed that the shape of the simulated pdf is close to the theoretical curve.

Moreover the agreement between the simulated and the theoretical improves when the

number of points is increased.

2.4.3 The Second-Order Statistics (Autocorrelation of $r(t)$)

The autocorrelation of $r(t)$ in continuous time domain is expressed as

$$E[r(t)r(t+\tau)] = \lim_{T\to\infty} \frac{1}{2T}\int_{-T}^{T} r(t)r(t+\tau)d\tau$$

$$\approx \frac{1}{2T}\int_{-T}^{T} r(t)r(t+\tau)d\tau \quad \text{when } T \text{ is large enough,}$$

while in discrete domain

$$E[r(n)r(n+i)] = \frac{1}{2M}\sum_{n=1}^{M} r(n)r(n+i) \tag{2.22}$$

The autocorrelation of $r(n)$ generated can be estimated by using the above function. It is reasonable to model $r(t)$ as a wide-sense stationary (WSS) stochastic process, which means the correlation properties do not depend on the time of observation, t and $t+\tau$, but only on their difference $\Delta t = \tau$. The normalized theoretical autocorrelation of $r(t)$ is given as [2]

$$\Phi_{rr}(\tau) = J_0(2\pi f_D \tau) \tag{2.23}$$

where $J_0(\bullet)$ represents zero$^{\text{th}}$ order Bessel function .

The degree of agreement between the simulated outcome and the theoretical values is illustrated in the Figure 2.10. As can be observed from the figure, the simulated results are very close to the theoretical curve for the first several fluctuations. However, the agreement becomes worse as the time difference increases.

2.5 Summary

In this chapter, a flat Rayleigh fading channel model is described in detail. We focus on the design and implementation of the Doppler filter. For computational convenience, we adopt *FFT* and *IFFT* to perform the convolution between the input signal and impulse response of Doppler filter. To verify the simulated signal, we analyze the simulated

outcome in the first order and second order statistics and compare them with the

theoretical curves. We find that the agreement is good. In the next Chapter we will

propose an improved search scheme which we need to build a simulator to obtain its

performance. The channel for the simulator is assumed to be flat Rayleigh fading. Hence

we generate this channel model to facilitate our further simulation in the following chapter.
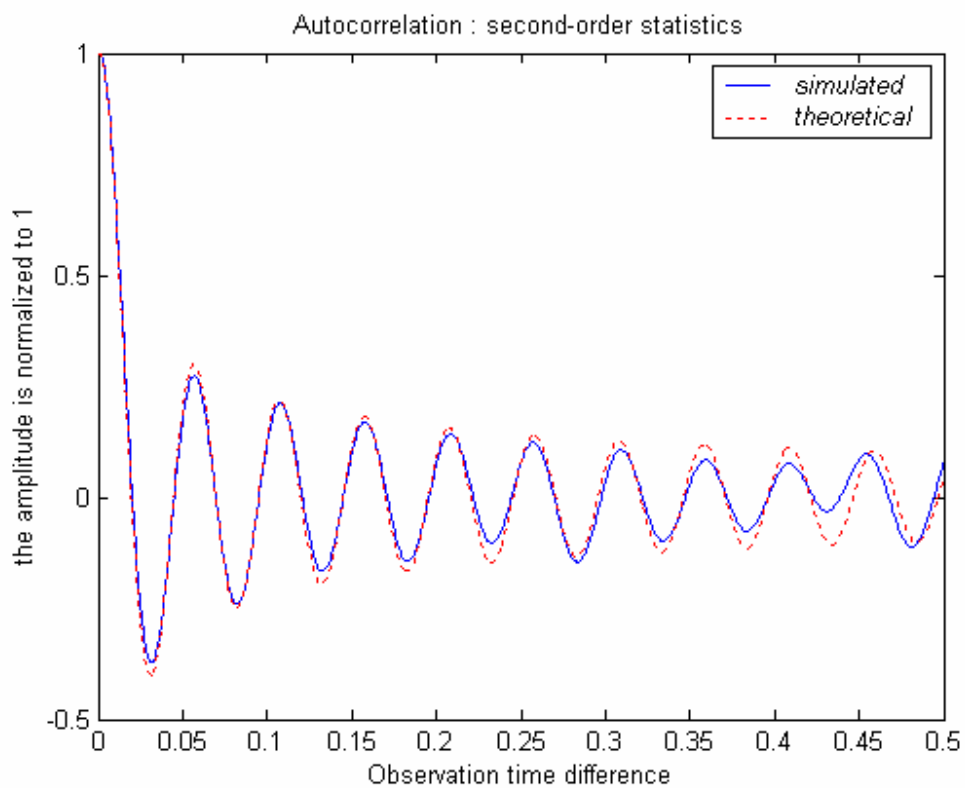
Figure 2.10   Autocorrelation of *r(t)*

Chapter 3 An Improved Rate Search Scheme for Multicode CDMA

Transmissions over Rayleigh fading mobile radio channels are subjected to error bursts due to deep fades, even when the channel signal-to-noise ratio (SNR) is high. This can be ameliorated through the use of power control whereby the transmitted rate is unchanged but the transmission level is adapted according to the channel integrity. However, this both increases transmitter power requirements, and more importantly increase the level of cochannel interference, which can severely curtail system's capacity. This leads people to the notion of varying the data rate according to the integrity of the channel, so that when the receiver is not in a fade we increase its transmitted rate, and as the receiver enters a fade we decrease its rate down to a value which maintains an acceptable quality of service (QoS).

3.1 Previous Works

"Adaptation" in the context of CDMA systems has long been mostly synonymous with power control which is used to overcome the famous near-far problem in order to increase the system's capacity. There have been a lot of existing works dealing with power control mechanism in CDMA systems [8][9]. This conventional way of power control ensures that all mobile signals are received with the same power. In current CDMA cellular systems, open loop and closed loop power control techniques are used in adjusting the

transmit power of each mobile. If the power control is perfect, then the channel appears to the transmitter and receiver as an AWGN channel. However, this scheme requires a large average transmit power to compensate for the deep fades. The compensation for the deep fades may appear as a strong interference to adjacent cells thereby decreasing the system's capacity. To avoid this, in [17] Kim and Goldsmith analyze the performance of truncated power control (TPC) on the assumption that the receiver can tolerate some delay. This power control scheme compensates for fading above a certain cutoff fade depth and silence the transmitter when fade depth is below the cutoff level. From the point of view of rate control, TPC can be viewed as a special case of joint rate and power adaptation in which there are only 2 rate states, fixed rate and silence.

In [15], Goldsmith and Chua explored a variable-rate and variable-power MQAM modulation for high-speed data transmission in which both the transmission rate and power are optimized to maximize spectral efficiency while satisfying the average power and BER constraints. The optimal adaptation strategy with a given set of rates requires choosing the optimal channel fade thresholds at which the user switches from one constellation to another. These thresholds divide the channel fade space into optimal rate regions. Since the transmit power is a function of just the required rate and the channel fade, power adaptation is fixed once the optimum rate adaptation is determined. Also this scheme exhibits a 5-10dB power gain relative to variable-power fixed-rate transmissions. However, it is only for a single user case and seems to be very little literature on the potential gains in a multi-user environment.

For the multiple access wireless channel the problem gets more interesting as users can interfere with each other. In [16], Chawla and Qiu proposed a general framework to study the performance of adaptive modulation in cellular systems, which provides valuable insight into the performance of the adaptive modulation in multi-user cellular systems. An iterative algorithm is proposed in the work to maximize the total transmission rate by maximizing the SIR values. Jafar and Goldsmith [18] proposed an optimal centralized adaptive rate and power control strategy to maximize the total average weighted throughput in a generic multirate CDMA system with slow fading. The result is general enough to apply to several multirate CDMA schemes: multi-code, multi-processing gain, multirate modulation or hybrids of these. In [19], Jafar and Goldsmith continued to put forward optimal strategies in a more specific Multicode CDMA for uplink throughput maximization. An upper bound to the maximum average throughput is obtained and evaluated for Rayleigh fading. Several cases are considered where the code rates available to each user are unlimited continuous, limited continuous and limited discrete respectively. In the case of limited discrete rates, the optimal rate searching scheme is not efficient in terms of search complexity. An improved method is proposed with lower search complexity.

3.2 System Model

Assume the system is a single cell, variable rate multicode CDMA system with K users, each having a specific assigned set of M code sequences. Peak power and instantaneous bit error rate (BER) constraints are assumed. The channel is affected by flat Rayleigh fading which is obtained from the simulation as previously described plus Additive White

Gaussian Noise (AWGN). Further assume that the receiver is able to estimate the channel state perfectly and a reliable feedback channel exists from the receiver to each of the transmitters for flow of rate and power control information. The channel fading gain changes at a rate slow enough for the delay on the feedback channel to be negligible. The code sequences assigned to a user are orthogonal so that a user does not interfere with himself. However, users do interfere with each other. i.e. sequences transmitted by different users are not orthogonal to each other. The system uses BPSK with coherent demodulation. The user's channel access is assumed to be asynchronous. The received signal at the base station is given as

$$s(t \mid \mathbf{G}) = \sum_{i \in I} \sum_{j=1}^{n_i(\mathbf{G})} \sqrt{\frac{2 S_i G_i}{n_i(\mathbf{G})}} a_{ij}(t - \tau_i) b_{ij}(t - \tau_i) \cos(\omega_c t + \Phi_i) + n(t), \qquad (3.1)$$

where $I = \{1, 2, \cdots K\}$ is the index set of users, $\mathbf{G} = (G_1, G_2, \cdots, G_K)$ is the vector of channel fade levels experienced by each user due to multipath, $\mathbf{n(G)} = (n_1, n_2, \cdots n_K)$ is the vector of codes transmitted, a_{ij}, b_{ij} are the data bit and code chip respectively, τ_i is the delay, S_i is the total transmitted power of the ith user. $n(t)$ is AWGN with two-sided power spectral density $\dfrac{N_0}{2}$. The received decision statistic after despreading for user i's j^{th} sequence becomes

$$z_{ij} = \sqrt{\frac{P_i(\mathbf{G})}{n_i(\mathbf{G})}} b_{ij} + \sum_{k \in I - \{i\}} \sum_{l=1}^{n_k} \sqrt{\frac{P_k(\mathbf{G})}{n_k(\mathbf{G})}} I_{ijkl} + n_{ij}, \qquad (3.2)$$

where I_{ijkl} is the multiple access interference term due to the interference between the ith user's j^{th} sequence and the kth user's l^{th} sequence. The variance of I_{ijkl} for random

bipolar rectangular chips is $\dfrac{1}{3N}$, where N is the processing gain. n_{ij} is the contribution

due to Gaussian noise and has a variance $\dfrac{N_o}{2T_b}$.

Under standard Gaussian approximation, the instantaneous BER can be expressed as [19],

$$BER = Q\left(\sqrt{2\left(\frac{E_b}{N_0} \right)} \right) \qquad (3.3)$$

where

$$\frac{E_b}{N_0} = \frac{P_i/n_i}{\dfrac{2}{3N} \displaystyle\sum_{k \in I-\{i\}} P_k + N_o/T_b} \qquad (3.4)$$

P_i : received power at base for user i

G_i : fade levels experienced by user i (flat fading)

S_i : transmitted power for user i

n_i : number of codes transmitted

N : spreading gain

N_o : single-sided power spectral density for AWGN

$I = \{1,2,\cdots K\}$ is the index set of users

Rewrite (3.4) as

$$n_i = \frac{P_i}{\sum_{k \in I - \{i\}} P_k + \frac{3NN_o}{2T_b}} \frac{3N}{(Q^{-1}(BER))^2}$$

$$= \frac{DP_i}{\sum_{k \in I - \{i\}} P_k + C}$$

(3.5)

where $C = \frac{3NN_o}{2T_b}$ and $D = \frac{3N}{(Q^{-1}(BER))^2}$ for notational convenience. n_i can be viewed

as the normalized bit rate for user i (normalize to $1/T_b$). The total instantaneous

throughput can be expressed as follows,

$$T(\mathbf{G}) = \sum_{k \in I} n_k(\mathbf{G}) = D \frac{P_i(\mathbf{G})}{\sum_{k \in I - \{i\}} P_k(\mathbf{G}) + C} \quad .$$

(3.6)

3.3 Original Optimal Adaptation Schemes

In [19] a series of schemes is provided to determine the maximum instantaneous total

throughput given that the fading vector $\mathbf{G}(G_1, G_2 \cdots G_K)$ is available and the rate vector

operates under various constraints.

3.3.1 Code Rate as an Unlimited Continuous Variable

When code rate n_i is treated as an unlimited continuous variable that takes values over the

entire range of positive real numbers, the optimal solution that maximizes the average

total throughput is such that [19]

$$P_k(\mathbf{G}) \in \{0, P_{k,\max}(G_i)\} \qquad \forall k \in I \ ,$$

where $P_{k,\max}(G_i) = G_i S_{i,\max}$. That is, either a user does not transmit, or he transmits at full power.

This optimal solution can be proved by differentiating (3.6) twice with respect to P_i.

$\dfrac{\partial^2 T}{\partial P_i^2}$ is found to be always positive. Hence $T(\mathbf{G})$ is a convex function of P_i and the maximum value will always lie at the boundary. Accordingly, the optimum instantaneous throughput is

$$T_{opt}(\mathbf{G}) = \sum_{i \in I_{opt}} n_i^c = D \sum_{i \in I_{opt}} \frac{P_{i,\max}(G_i)}{\sum_{k \in I_{opt}-\{i\}} P_{k,\max}(G_k) + C} \ , \tag{3.7}$$

and the optimum rate vector as $\mathbf{n} = (n_1^c, n_2^c, \cdots n_{k_{opt}}^c, 0, \cdots 0)$. $I_{opt} = \{1, 2, \cdots k_{opt}\} \subset I$ is the set of users transmitting at their peak powers for maximum throughput. Note that here the peak received powers for each user is sorted according to

$$P_{i,\max}(G_i) \ge P_{j,\max}(G_j) \quad \forall i < j \,.$$

k_{opt} is the minimum number of users that need to transmit simultaneously to achieve the maximum possible throughput.

Hence the optimum unlimited continuous rate and power adaptation scheme is as follows: Firstly find the throughputs achieved by the n best users transmitting at their peak transmit powers as

$$T_n = D \sum_{i=1}^{n} \frac{P_{i,\max}(\mathbf{G})}{\sum_{k \in I_{opt}-\{i\}} P_{k,\max}(\mathbf{G}) + C} \quad 1 \le n \le K \,. \tag{3.8}$$

Secondly, choose the maximum T_n as T_{opt}.

$$T_{opt}(\mathbf{G}) = \max_{1 \le n \le K} T_n(\mathbf{G})$$

T_n can be evaluated with complexity $\sim O(K)$ for each n. Thus the optimum rates and

powers are found with a computational complexity $\sim O(K^2)$ [19].

3.3.2 Code Rate as a Limited Discrete Variable

Before we start discussing the improved search scheme, it is necessary for us to take a

look at the original scheme's mechanism. In this section we will review the original search

scheme which is already fully described in [19]. The number of codes available to each

user is constrained to be positive integer values less than or equal to M. The received

signal powers required to achieve a rate vector $\mathbf{n}(n_1, n_2, \cdots, n_k)$ can be expressed as [19]

$$P_i(\mathbf{G}) = C\left(\frac{n_i}{n_i + D}\right)\frac{1}{1-\gamma} \quad \forall i \in I \tag{3.9}$$

where $\gamma = \sum_{j \in I} \dfrac{n_j}{n_j + D}$.

Obviously, using $P_i = G_i S_i$ and the peak power constraint S_{max}, it is obvious that

$$P_i \le G_i S_{max}. \tag{3.10}$$

Substituting (3.10) into (3.9), we obtain the fading vector as [19]:

$$G_i \ge \frac{C}{S_{max}}\left(\frac{n_i}{n_i + D}\right)\frac{1}{1-\gamma} \quad \forall i \in I \tag{3.11}$$

where rate vector $\mathbf{n}(n_1, n_2, \cdots, n_k)$ is restricted to discrete integer numbers.

This leads to the optimum rate and power adaptation scheme as follows.   For every

achievable rate vector **n,** there is a corresponding channel fade vector **G** such that

$$G_i = \frac{C}{S_{\max}} \left(\frac{n_i}{n_i + D} \right) \frac{1}{1-\gamma},$$
(3.12)

and a corresponding throughput $T(\mathrm{n}) = \sum_{i \in I} n_i$. Arrange all achievable rate vectors and

channel fade vectors into a table in increasing order of the corresponding throughputs.

This table is illustrated as follows.

l	$\mathbf{n}(l)$	$\mathbf{G}(l)$	$T(l)$
1	$\{n_1(1), n_2(1), \cdots, n_k(1)\}$	$\{G_1(1), G_2(1), \cdots G_K(1)\}$	$\sum n_i(1)$
2	$\{n_1(2), n_2(2), \cdots, n_k(2)\}$	$\{G_1(2), G_2(2), \cdots G_K(2)\}$	$\sum n_i(2)$
3	$\{n_1(3), n_2(3), \cdots, n_k(3)\}$	$\{G_1(3), G_2(3), \cdots G_K(3)\}$	$\sum n_i(3)$
$\vdots$	$\vdots$	$\vdots$	$\vdots$

Table 3.1   Sorted Fade and Rate Vectors List

For a given fading vector $\mathbf{G}(G_1, G_2 \cdots G_K)$, the optimum throughput, and rate can be

found by searching Table 3.1.   Check all achievable rate vectors that satisfy (3.11) and

choose the one with the maximum total throughput $T(\mathbf{n}) = \max\left(\sum_{i \in I} n_i(l) \right)$ as the optimal

rate vector. However, this poses a problem. The size of search table can be extremely high

due to the large number of the achievable vectors. It is shown in Table 3.2 that the number

of the achievable vector increases almost exponentially as the maximum achievable total

achievable throughput $T_{\max}$ and number of users K increases.

3.4 Motivation of the Improved Search Scheme

In [19], when the code rates available to each user are limited to be discrete integers,

searching for the optimal rate vector become very cumbersome. The original scheme is

described as follows. Firstly, arrange all possible achievable rate vectors into a table in

increasing order of the corresponding throughputs. Secondly, check all the rate vectors

that satisfy Equation (3.11) in the system given the channel fading information **G**. Select

the rate vector with the maximum summation as the optimal rate vector. For convenience,

we define the maximum number of achievable rate vectors that need to be checked as

search complexity. For the case of the original search approach, the search complexity

refers to the size of the search table. The size of the search table obviously depends on the

number of users K in the system, the maximum total achievable throughput T and the

code rate quota M . The problem for the original approach is that search complexity might

be very high which causes the searching inefficient especially in the case when the

maximum achievable throughput is relatively large. Another problem is that the available

code rates have to be limited within a full quota M. M cannot be infinite due to the reason

that when the maximum rate becomes infinite, the number of achievable rate vectors goes

to infinity almost exponentially. The following table represents a case showing how the

search complexities increase as the maximum total achievable throughput T increases.

Taking K=10 and T=40 for example, the number of achievable rate vectors can be 115304,

which is a very large search number. Hence the need to find less complex search

mechanism motivates us to further explore an improved scheme so that the search complexity would be reduced and the value of full rate quota M can be loosed to be any positive discrete number without sacrificing on the system's performance.

Number of users K	10	10	10
Maximum total achievable throughput T	20	30	40
Size of the search table (search complexity)	2429	20544	115304

Table 3.2   Size of the Search Table

3.5   Improved Search Scheme

Firstly, let us define the optimal rate vector. We assume that the optimal rate vector is denoted by $\mathbf{n}(n_1, n_2, \cdots n_K)$. Then $\mathbf{n}$ must satisfy (3.11) and $\sum n_i$ is maximal among all achievable vectors. For convenience, $\mathbf{n}$ can be sorted as $n_i \geq n_{i+1}$ and $\mathbf{G}(G_1, G_2, \cdots G_K)$ be sorted as $G_i \geq G_{i+1}$. It is also worth mentioning that it is possible that there are more than one rate vectors with the same maximum summation. For example, it is possible for both $(n_1, n_2 \cdots n_k)$ and $(n_1, n_2, \cdots n_i + 1, n_{i+1}, \cdots, n_j - 1, n_{j+1}, \cdots n_k)$ $\forall i < j$ to satisfy (3.11). Under such a situation, we will consider that the second vector is better than the first although their summations are the same. The reason is that the second vector results in less MAI . With the definition above, there is just one optimal vector in the system once the fading vector $\mathbf{G}$ is known.

3.5.1 The Rate Full Quota M as Unlimited Positive Integer

Further, we find that the optimal rate vector must follow some additional conditions shown in (3.14). Assume $\mathbf{n}(n_1, n_2, \cdots n_k)$ is the optimal maximum rate vector for fading vector in which n_i can take any value of positive integer. $\mathbf{G}(G_1, G_2, \cdots G_k)$ is channel information. And we further assume that there are h out of K users that are non-zeros in vector $\mathbf{n}$. Hence, the rate vector $\mathbf{n}(n_1, n_2, \cdots n_k)$ can be further expressed as

$$\mathbf{n}(\underbrace{n_1, n_2, \cdots n_h}_{h}, \underbrace{0, \cdots, 0}_{K-h}) . \tag{3.13}$$

Note that we have sorted $\mathbf{n}$ as $n_i \geq n_{i+1}$ $\forall i \in I$. So we have h users transmitting at rates of at least 1 and the remaining $K - h$ users are silent. For $\mathbf{n}$ to be an optimal maximum rate vector, the following must hold true,

$$G_i \leq \frac{C}{S_{\max}} \left(\frac{n_i + 1}{n_i + 1 + D} \right) \frac{1}{1 - \gamma^i} \qquad \forall i < h \tag{3.14}$$

where γ^i is similar to γ in (3.11) while replacing the two terms $\dfrac{n_i}{n_i + D}$, $\dfrac{n_h}{n_h + D}$ in γ

with $\dfrac{n_i + 1}{n_i + 1 + D}$, $\dfrac{n_h - 1}{n_h - 1 + D}$ respectively. It is true that

$$\gamma^i \leq \gamma . \tag{3.15}$$

Proof of (3.15):

Assume that rate vector $\mathbf{n} = (n_1, n_2, \cdots, n_h, 0, 0, \cdots, 0)$ is the optimal rate vector. Then we

define $\gamma = \sum\limits_{i=1}^{h} \dfrac{n_i}{n_i + D}$. We can obtain $\mathbf{n}^i$ by increasing n_i by 1 ($\forall i < h$) and decreasing n_h

by 1 in the vector $\mathbf{n}$. Hence $\mathbf{n}^i = (n_1, n_2, \cdots n_{i-1}, n_i + 1, n_{i+1}, \cdots, n_h - 1, 0, 0, \cdots 0)$. γ^i is

something similar to γ. The difference between γ^i and γ is that the term $\dfrac{n_i}{n_i + D}$ and

$\dfrac{n_h}{n_h + D}$ in γ are replaced with $\dfrac{n_i + 1}{n_i + 1 + D}$ and $\dfrac{n_h - 1}{n_h - 1 + D}$ respectively. The rest is the

same. Therefore, to compare γ^i and γ is to compare $\dfrac{n_i + 1}{n_i + 1 + D} + \dfrac{n_h - 1}{n_h - 1 + D}$ with

$\dfrac{n_i}{n_i + D} + \dfrac{n_h}{n_h + D}$. Remember that we have sorted the rate vector $\mathbf{n}$ as $n_i \geq n_j \quad \forall i < j$, namely

$n_i \geq n_h \quad \forall i < h$. It is obvious that $\dfrac{n_i + 1}{n_i + 1 + D} + \dfrac{n_h - 1}{n_h - 1 + D} \leq \dfrac{n_i}{n_i + D} + \dfrac{n_h}{n_h + D}$ when

$n_i \geq n_h$. So we have $\gamma^i \leq \gamma$. This completes the proof.

Proof of (3.14):

Suppose the index $i = 1$ and rate vector $\mathbf{n}$ $(n_1, n_2, \cdots n_h, 0, \cdots 0)$ is the optimal rate vector.

We generate an alternative rate vector as follows,

$$\mathbf{n}^1 = (n_1^1, n_2^1, \cdots n_h^1, 0, 0, \cdots 0) \tag{3.16}$$

where

$$n_k^1 = \begin{cases} n_k & k \neq 1, h \\ n_k + 1 & k = 1 \\ n_k - 1 & k = h \end{cases} \tag{3.17}$$

We define $\gamma^1 = \displaystyle\sum_{j=1}^{h} \dfrac{n_j^1}{n_j^1 + D}$ and $\gamma = \displaystyle\sum_{j=1}^{h} \dfrac{n_j}{n_j + D}$

From the assumption that $\mathbf{n}$ is the optimal rate vector, we have

$$G_a \geq \frac{C}{S_{\max}} (\frac{n_a}{n_a + D}) \frac{1}{1-\gamma} \qquad \forall a \leq h$$

When the rate vector in the system is $\mathbf{n}$, the total received power of user 1 and user h is denoted as $P_1(\mathbf{n}) + P_h(\mathbf{n})$. If we increase n_1 by 1 and decrease n_h by 1, the rate vector in the system become $\mathbf{n}^1$ and total received power of user 1 and user h is denoted as $P_1(\mathbf{n}^1) + P_h(\mathbf{n}^1)$. According to the proof of proposition 3 at page 8 in [19], if $G_1 \geq G_h$, we have

$$P_1(\mathbf{n}^1) + P_h(\mathbf{n}^1) \leq P_1(\mathbf{n}) + P_h(\mathbf{n}) \tag{3.18}$$

(3.18) tell us that the rate change in user 1 and user h reduce MAI to the remaining users. In other words, the current channel condition is enough to support the rates of users (other than user 1 and user h), namely

$$G_a \geq \frac{C}{S_{\max}} \left(\frac{n_a^1}{n_a^1 + D} \right) \frac{1}{1-\gamma^1} \quad \forall a \leq h \ \& \ a \neq i, h \tag{3.19}$$

In addition, the rate of user h is reduced by 1, obviously the channel condition of user h will support its rate, namely

$$G_h \geq \frac{C}{S_{\max}} \left(\frac{n_h^1}{n_h^1 + D} \right) \frac{1}{1-\gamma^1} \tag{3.20}$$

now we only have user 1 left .   If

$$G_1 \geq \frac{C}{S_{\max}} \left(\frac{n_1^1}{n_1^1 + D} \right) \frac{1}{1-\gamma^1} \ , \tag{3.21}$$

then (3.11) will be true for rate vector $\mathbf{n}^1$. Apparently this will contradict our assumption that rate vector $\mathbf{n}$ is the optimal rate vector. Therefore

$$G_1 < \frac{C}{S_{\max}} \left(\frac{n_1^1}{n_1^1 + D} \right) \frac{1}{1 - \gamma^1} \tag{3.22}$$

Similarly, We can get the same conclusion when $i = 2, 3, \cdots, h - 1$.

Hence,

$$G_i < \frac{C}{S_{\max}} \left(\frac{n_i^i}{n_i^i + D} \right) \frac{1}{1 - \gamma^i} \qquad \forall i < h \tag{3.23}$$

Since $n_i^i = n_i + 1$ (See (3.17)), (3.23) can be rewritten as follows,

$$G_i \le \frac{C}{S_{\max}} \left(\frac{n_i + 1}{n_i + 1 + D} \right) \frac{1}{1 - \gamma^i} \quad \forall i < h \tag{3.14}$$

End of proof for (3.14)

Equation (3.11) and (3.14) enable us to narrow down the search range of the optimal vector to avoid searching all possible vectors. Suppose that the h users transmit at maximum power of $S_{\max}$ and the number of codes can be continuously varied. Then we have

$$G_i = \frac{C}{S_{\max}} \frac{n_i^c}{n_i^c + D} \frac{1}{1 - \gamma^c} \qquad \forall i \le h \tag{3.24}$$

where n_i^c is continuously varied and $n_i^c = \dfrac{DG_i S_{\max}}{\sum_{k = I - \{i\}} G_k S_{\max} + C}$, $\gamma^c = \sum_{j \le h} \dfrac{n_j^c}{n_j^c + D}$.

With (3.11), (3.14) and (3.24), we have

$$n_i \ge \lfloor n_i^c \rfloor \qquad \forall i < h \tag{3.25}$$

$$n_h \le \lceil n_h^c \rceil \tag{3.26}$$

where $\lfloor x \rfloor$ is the largest integer less than x and $\lceil x \rceil$ is the smallest integer more than x.

Proofs of (3.25) and (3.26) are presented as follows.

Proof of (3.25):

$$n_i \geq \lfloor n_i^c \rfloor \qquad\qquad \forall i < h$$

Start with (3.11): $$G_i \geq \frac{C}{S_{max}} \left(\frac{n_i}{n_i + D} \right) \frac{1}{1 - \gamma} \qquad \forall i \in I$$

Rearranging terms, we have

$$\frac{n_i}{n_i + D} \leq \frac{G_1 S_{max} (1 - \gamma)}{C} .$$

From the definition of γ in (3.9), we obtain

$$\gamma = \sum_{i=1}^{K} \frac{n_i}{n_i + D} \leq \frac{S_{max}(1 - \gamma)}{C} \sum_{i=1}^{K} G_i$$

$$\Rightarrow \; \gamma \leq \frac{S_{max} \sum_{i=1}^{K} G_i}{S_{max} \sum_{i=1}^{K} G_i + C} . \qquad\qquad (3.27)$$

Using equation (3.14), we get

$$G_i \leq \frac{C}{S_{max}} \left(\frac{n_i + 1}{n_i + 1 + D} \right) \frac{1}{1 - \gamma^i} \qquad \forall i < h$$

Rearranging terms, we have

$$n_i + 1 \geq \frac{D \dfrac{G_i S_{max}}{C} (1 - \gamma^i)}{1 - \dfrac{G_i S_{max}}{C} (1 - \gamma^i)} .$$

Given that $y' \leq \gamma$ (3.15), we have

$$n_i + 1 \geq \frac{D \dfrac{G_i S_{max}}{C}(1-\gamma)}{1 - \dfrac{G_i S_{max}}{C}(1-\gamma)} \, .$$

Then, from equation (3.27), we have

$$n_i + 1 \geq \frac{D \dfrac{G_i S_{max}}{C}\left(1 - \dfrac{S_{max}\sum\limits_{i=1}^{K} G_i}{S_{max}\sum\limits_{i=1}^{K} G_i + C}\right)}{1 - \dfrac{G_i S_{max}}{C}\left(1 - \dfrac{S_{max}\sum\limits_{i=1}^{K} G_i}{S_{max}\sum\limits_{i=1}^{K} G_i + C}\right)} = \frac{D G_i S_{max}}{\sum_{I-\{i\}} G_i S_{max} + C} = n_i^c$$

$$\Rightarrow \ n_i + 1 \geq n_i^c$$

$$\Rightarrow \ n_i \geq \left\lfloor n_i^c \right\rfloor$$

End of proof for (3.25)

Proof of (3.26):

$$n_h \leq \left\lceil \ n_h^c \ \right\rceil$$

Suppose that rate vector $\mathbf{n} \ (n_1, n_2, \cdots n_h, 0, \cdots 0)$ is the optimal rate vector and we sort $\mathbf{n}$ as

$n_i \geq n_j \quad \forall i < j$. The corresponding transmitted power vector for the rate vector $\mathbf{n}$ is

denoted as $\mathbf{S} \ (S_1, S_2, S_3, \cdots, S_h, 0, \cdots, 0)$ where $S_i \leq S_{max}$, $\forall i \leq h$.

The relationship between rate and fading is given as [19]:

$$P_i = G_i S_i = C\left(\frac{n_i}{n_i + D}\right)\frac{1}{1-\gamma}$$

$$\Rightarrow \quad G_i = \frac{C}{S_i}\left(\frac{n_i}{n_i + D}\right)\frac{1}{1-\gamma} \tag{3.28}$$

Consider a scenario where (3.16) is not true by assuming $n_h = \left\lceil n_h^c \right\rceil + 1$.

According to (3.24), we have

$$n_h^c = \frac{D G_h S_{\max}}{\sum_{k<h} G_k S_{\max} + C} \ . \tag{3.29}$$

If $n_h = \left\lceil n_h^c \right\rceil + 1$, then

$$n_h = \left\lceil n_h^c \right\rceil + 1 = \frac{D G_h S_h}{\sum_{k<h} G_k S_k + C} \ . \tag{3.30}$$

Dividing (3.29) by (3.30), we obtain

$$\frac{n_h^c}{\left\lceil n_h^c \right\rceil + 1} = \frac{\sum_{k<h} G_k S_k + C}{\sum_{k<h} G_k S_{\max} + C} \frac{S_{\max}}{S_h} \ . \tag{3.31}$$

Since user h's transmitted power S_h is upper bounded by peak power constraint $S_{\max}$, it is

obvious that the term $\dfrac{S_{\max}}{S_h}$ is equal to or larger than 1.

$$\frac{n_h^c}{\left\lceil n_h^c \right\rceil + 1} \geq \frac{\sum_{k<h} G_k S_k + C}{\sum_{k<h} G_k S_{\max} + C}$$

$$\Rightarrow \quad \frac{n_h^c}{\left\lceil n_h^c \right\rceil + 1} \geq \frac{\sum_{k<h} G_k S_k}{\sum_{k<h} G_k S_{\max}} \tag{3.32}$$

With equation (3.14) and (3.28)

$$\begin{cases} G_i = \dfrac{C}{S_i}\left(\dfrac{n_i}{n_i + D}\right)\dfrac{1}{1-\gamma} \ldots\ldots\ldots\ldots(3.28) \\[3mm] G_i < \dfrac{C}{S_{max}}\left(\dfrac{n_i + 1}{n_i + 1 + D}\right)\dfrac{1}{1-\gamma^i} \ldots\ldots(3.14) \end{cases},$$

the relationship for the right hand side parts of both equations can be expressed as follows:

$$\frac{C}{S_i}\left(\frac{n_i}{n_i + D}\right)\frac{1}{1-\gamma} < \frac{C}{S_{max}}\left(\frac{n_i + 1}{n_i + 1 + D}\right)\frac{1}{1-\gamma^i}.$$

Rearranging terms, we obtain

$$\frac{S_i}{S_{max}} > \frac{n_i}{n_i + D}\,\frac{n_i + 1 + D}{n_i + 1}\,\frac{1-\gamma^i}{1-\gamma},$$

where term $\dfrac{1-\gamma^i}{1-\gamma}$ is equal to or greater than 1 by using the conclusion $\gamma^i \le \gamma$ (3.15).

Then,

$$\frac{S_i}{S_{max}} > \frac{n_i}{n_i + 1}\,\frac{n_i + 1 + D}{n_i + D}$$

$$\Rightarrow \qquad \frac{S_i}{S_{max}} > \frac{n_i}{n_i + 1}$$

As we previously stated that rate codes in the rate vector **n** were so sorted as $n_i \ge n_j \forall i < j$,

we have

$$\frac{n_i}{n_i + 1} \ge \frac{n_{h-1}}{n_{h-1} + 1} \qquad \forall i < h.$$

Hence,

$$\frac{S_i}{S_{max}} > \frac{n_{h-1}}{n_{h-1} + 1} \quad \forall i < h. \tag{3.33}$$

According to (3.33), the right hand side of (3.32) can be lower bounded by following:

$$\frac{\sum_{k<h} G_k S_k}{\sum_{k<h} G_k S_{\max}} > \frac{\sum_{k<h} G_k S_{\max} \frac{n_{h-1}}{n_{h-1}+1}}{\sum_{k<h} G_k S_{\max}} = \frac{n_{h-1}}{n_{h-1}+1}$$

$$\Rightarrow \quad \frac{\sum_{k<h} G_k S_k}{\sum_{k<h} G_k S_{\max}} > \frac{n_{h-1}}{n_{h-1}+1} \tag{3.34}$$

$$\because \quad \frac{n_{h-1}}{n_{h-1}+1} \geq \frac{n_h}{n_h+1} > \frac{n_h^c}{\left\lceil n_h^c \right\rceil +1} \quad \text{(Note that } n_h = \left\lceil n_h^c \right\rceil + 1 \text{)}$$

It can be seen that (3.34) contradicts with (3.32), which indicates our assumption about

$n_h = \left\lceil n_h^c \right\rceil + 1$ is incorrect.

Similarly, we can obtain the same conclusion when we set

$n_h = \left\lceil n_h^c \right\rceil + 2, \left\lceil n_h^c \right\rceil + 3, \left\lceil n_h^c \right\rceil + 4, \cdots$

Therefore,

$$n_h \leq \left\lceil n_h^c \right\rceil$$

End of proof for (3.26)

We have therefore narrowed down the range of the optimal rate using (3.25) and (3.26).

Our proposed scheme works as follows. The possible values for h range from 1 to K, and

the possible values for n_h range from 1 to $\left\lceil n_h^c \right\rceil$.

Step 1: Set the initial rate vector state as

$$n_i = \left\lfloor n_i^c \right\rfloor \qquad \forall i < h$$

$$n_h = 1$$

Step 2:　Add 1 to n_j where j is the index that yields the minimum of the following

relationship

$$\frac{\dfrac{n_j+1}{n_j+1+D}\dfrac{1}{1-\gamma'}}{\dfrac{n_j^c}{n_j^c+D}\dfrac{1}{1-\gamma^c}} \qquad (3.35)$$

namely,

$$\frac{\dfrac{n_j+1}{n_j+1+D}\dfrac{1}{1-\gamma^j}}{\dfrac{n_j^c}{n_j^c+D}\dfrac{1}{1-\gamma^c}} \leq \frac{\dfrac{n_i+1}{n_i+1+D}\dfrac{1}{1-\gamma^i}}{\dfrac{n_i^c}{n_i^c+D}\dfrac{1}{1-\gamma^c}} \qquad \forall i \leq h$$

(3.35) is obtained by dividing the right hand side of (3.14) by the right hand side of (3.15).

The numerator in (3.35) is larger than the denominator if the vector is optimal. Since the

element with minimum value of (3.35) is most likely underestimated, this element can

possibly be increased by one. Then the vector state is changed from the initial one to the

new state with the element j incremented by 1.

Repeat step 2 until the minimum of (3.35) is larger than or equal to 1, or the current vector

state does not satisfy (3.11). For the first case, we will get a valid vector because this rate

vector satisfies both (3.11) and (3.14). For the second case, it is not a valid rate vector

since we cannot find a rate vector satisfying both (3.11) and (3.14). Note that the number

of times step 2 is repeated will not be larger than h. This is because the maximum

instantaneous throughput is between $\sum_{i \leq h} \left\lceil n_i^c \right\rceil$ and $\sum_{i \leq h} \left\lfloor n_i^c \right\rfloor$.

Step 3: In Step 2 , we set $n_h = 1$ which actually is ranging from 1 to $\left\lceil n_h^c \right\rceil$. Hence, we

need to try out every possible value for n_h and repeat Step 1 and Step 2.

Step 4: Things are similar with the case of n_h. Check every possible value of h ranging

from 2 to number of user K by repeating Step 1, 2 and 3. For the case of $h = 1$, only one

step was involved . Namely, $T = \left\lfloor n_1^c \right\rfloor$.

Step 5: We can obtain many valid rate vectors by trying all the possible values for each

n_h and h . Choose the one with maximum T .

We illustrate this with a simple example. Suppose h=3 and fade vector $\mathbf{G} = (2.9401,$

2.3971, 1.9654).

Step 1: Initial vector state is: ($\left\lfloor n_1^c \right\rfloor, \left\lfloor n_2^c \right\rfloor, 1$)=(5,4,1) . Check this vector with (3.11), find

that (3.11) is true. So the initial vector is (5, 4, 1).

Step 2: Compute (12) , we obtain (0.8628, 0.9351). The 1st one is the minimum. Add 1 to

the 1st user and the vector state become (6 , 4, 1). Check this vector with (3.11) and

find that (3.11) holds true. The vector state remains as (6, 4, 1).

Repeat step 2: Computing (3.35) gives (0.9593, 0.9351). The 2nd one is the minimum. Add

1 to the 2nd user and the vector state changes to (6, 5, 1). Check this vector state

with (3.11) and observe that (3.11) is not true. So the vector state is invalid and

simply drop it.

Try the next value of n_h by setting the initial vector state as : $(\lfloor n_1^c \rfloor, \lfloor n_2^c \rfloor, 2) = (5,4,2)$.

Following Step 1 and 2 above, we will end up with an invalid vector (6, 5, 2) and so drop

it.

Reset the initial vector state as: $(\lfloor n_1^c \rfloor, \lfloor n_2^c \rfloor, 3) = (5,4,3)$. Following Steps 1 and 2 above, we

will obtain a valid vector (6, 4, 3). Hence the optimal rate vector is (6, 4, 3) for $h = 3$. In

this example, we get only one valid rate vector. It is worth mentioning that we can get

more than one valid vectors. In that case, choose the one with maximum T.

3.5.2 The Rate Full Quota M as Limited Positive Integer

Previously, we have explored the case where M can be any positive discrete numbers.

The initial rate states are given in (3.25) and (3.26). However, in practical systems, the

rate full quota M is limited to be a certain number. In this case, the basic searching

principle remains the same but the search scheme is slightly different from the previous

case.

Now we further assume that the rate is limited to be an integer between 0 and M. We

continue to apply the scheme to this case only with little modification. As before, we

assume   that   the   optimal   rate   vector   is   n $= (n_1, n_2, \cdots, n_h, 0, 0, \cdots, 0)$ and

$n^c = (n_1^c, n_2^c, \cdots, n_h^c, 0, 0, \cdots 0)$ is the corresponding continuously varied rate vector.

Supposing that $n_i^c \geq M$ for all $i \leq b$, we can limit the optimal rates' range as follows.

$$n_i = M \qquad\qquad i \leq b \qquad\qquad\qquad\qquad (3.36)$$

$$n_i \geq \lfloor n_i^c \rfloor \qquad\qquad b < i < h \qquad\qquad\qquad\qquad (3.37)$$

$$. \qquad\qquad n_h \leq M \qquad\qquad i = h \qquad\qquad\qquad\qquad (3.38)$$

The validity of (3.36) and (3.37) can be easily seen from (3.25) in this report and our assumption that $n_i^c \geq M$ for all $i \leq b$. (3.38) is according to the M discrete set of rate assumption. Similarly, this leads to the optimum rate and power adaptation as follows:

Step1: Set the initial rate vector state as

$$\begin{cases} n_i = \min(M, \lfloor n_i^c \rfloor) & 1 \leq i < h - 1 \\ n_i = 1 & i = h \end{cases}$$

Step 2: Suppose b is the index such that $n_i = M$ for $i \leq b$ where $1 \leq b < h$. Since n_i already reaches its rate limit, it is unnecessary to adjust the value of n_i for $i \leq b$. What we need to do is to adjust the value of n_i for $b < i < h$. The way we adapt the current vector state to the optimum rate vector state is the same as the previous case and it is presented as follows:

Add 1 to n_j where j is the index that yields the minimum of the following relationship

$$\frac{\dfrac{n_j + 1}{n_j + 1 + D} \dfrac{1}{1 - \gamma^j}}{\dfrac{n_j^c}{n_j^c + D} \dfrac{1}{1 - \gamma^c}} \leq \frac{\dfrac{n_i + 1}{n_i + 1 + D} \dfrac{1}{1 - \gamma^i}}{\dfrac{n_i^c}{n_i^c + D} \dfrac{1}{1 - \gamma^c}} \qquad \forall b < i < h$$

where n_i^c , γ^i and γ^c are given in a form as the case where there is no rate range limit.

In case that the value of n_j reaches the rate bound M, b need to be incremented by 1

because b is used to record the number of user who has reach the rate limit. Then the rate

vector state is changed from

$$\mathbf{n} = \left(\underbrace{M, M, \cdots M}_{i \le b}, \underbrace{\lfloor n_{b+1} \rfloor \lfloor n_{b+2} \rfloor \cdots \lfloor n_{h-1} \rfloor}_{b < i < h}, \underbrace{1}_{i=h}, 0, 0, \cdots 0 \right)$$

to

$$\mathbf{n} = \left(\underbrace{M, M, \cdots M}_{i \le b}, \underbrace{\lfloor n_{b+1} \rfloor \lfloor n_{b+2} \rfloor, \cdots, \lfloor n_j \rfloor + 1, \cdots \lfloor n_{h-1} \rfloor}_{b < i < h}, \underbrace{1}_{i=h}, 0, 0, \cdots 0 \right)$$

Repeat step 2 until the minimum of the above relationship is larger than or equal to 1 or

the equation (3.11) is not satisfied.

Step 3: n_h ranges from 1 to $\min(O, M)$ where O is a number such that for any positive

integer $n_h \le O$, vector $(n_1, n_2, \cdots, n_h, 0, \cdots, 0)$ always satisfies (3.11) . Fortunately, in most

cases O is always less than M which can be reflected in the simulation results.

Step 4 and 5 are the same with the previous case.

3.6   Search Complexity of The Improved Scheme

Search complexity of the scheme analysis is as follows. As mentioned above, the

achievable total instantaneous throughput is between $\sum_{i \le h} \lceil n_i^c \rceil$ and $\sum_{i \le h} \lfloor n_i^c \rfloor$ for each

h and the gap in between is $\sum_{i\leq h}\left\lceil n_i^c \right\rceil$ - $\sum_{i\leq h}\left\lfloor n_i^c \right\rfloor = h$. Then there are λ steps of

vector state adaptation for each h and n_h. Due to the fact that the maximum achievable

instantaneous throughput is $\sum_{i\leq h}\left\lceil n_i^c \right\rceil$ and the initial searching rate vector is

$\left(\left\lfloor n_1^c \right\rfloor, \left\lfloor n_2^c \right\rfloor, \cdots, \left\lfloor n_{h-1}^c \right\rfloor, n_h, 0, \cdots, 0\right)$. Therefore the instantaneous throughput is $\sum_{i<h}\left\lfloor n_i^c \right\rfloor + n_h$,

obviously the upper bound for λ is

$$\sum_{i\leq h}\left\lceil n_i^c \right\rceil - \sum_{i<h}\left\lfloor n_i^c \right\rfloor + n_h = h + \left\lfloor n_h^c \right\rfloor - n_h .$$

The searching complexity for each rate vector is then

$$\sum_{h=2}^{K} \sum_{n_h=1}^{\left\lceil n_h^c \right\rceil} \left[h + \left\lfloor n_h^c \right\rfloor - n_h \right] + 1 . \tag{3.39}$$

Firstly, as can be seen from (3.39), the searching complexity is independent of the

maximum achievable throughput but the number of user K affect the searching steps. The

simulation results also support the above conclusions. Secondly, the searching complexity

of the scheme is far less than the original one in which the size of the searching table

would become extremely large as a result of large maximum achievable throughput [19].

Since it is very difficult to obtain numerical result of the complexity, we will illustrate the

complexity improvement by evaluating the average searching steps through simulation.

Both cases (unlimited M and limited M) are simulated to show the search complexity of

this search scheme. The source codes are available in Appendix C. The basic simulation

parameters are given as: Spreading Gain N=63, $D = \dfrac{3N}{\left(Q^{-1}(BER)\right)^2} = 20$, $\dfrac{E_b}{N_o} = 12dB$.

Channel power fade are assumed to be flat Rayleigh fading.   With these parameters, the maximum number of users that can transmit simultaneously is $K = 10$. For the case that rates available to each user are restricted to be a limited discrete integer, users are allowed to transmit from 5 to 15 codes. Table 3.3 shows the average steps of searching state transformations given the number of users and maximum achievable throughput in this new scheme. We can find that the searching complexity is greatly reduced especially when the maximum achievable throughput is large.

The average search steps under different M are found and plotted from Figure 3.1 to Figure 3.4. The curve suggests that for the original scheme, the search complexity rise dramatically as the maximum achievable throughput T_{max} increases while for the proposed scheme, it only increases slightly. We also observe from the plots that M can affect the original search complexity. Hence, the larger the M is, the more significant the improvement we can receive from the scheme.

Number of users K	10	10	10
Maximum achievable total throughput T	20	30	40
Search complexity of original scheme in [19]	2429	20544	115304
Average searching steps of proposed scheme	30.71	32.12	31.77

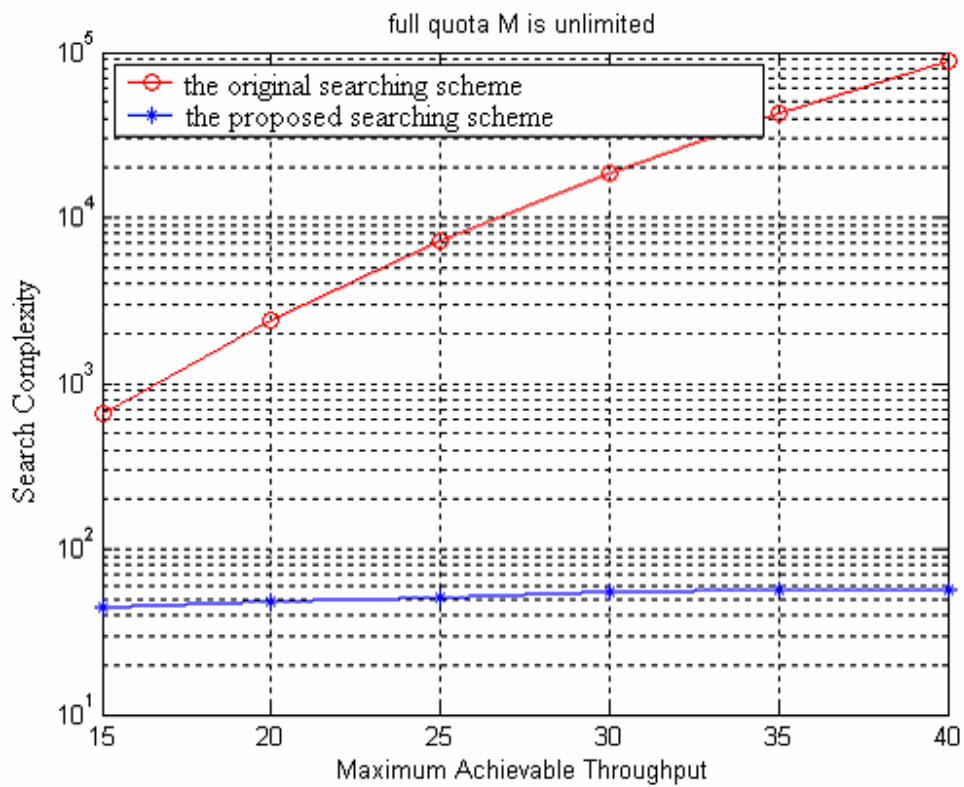**Table 3.3   Comparison of the Effects of the Two Schemes**

Figure 3.1   The Effects of Two Schemes Under Various $T\max$ (*M* no limit)
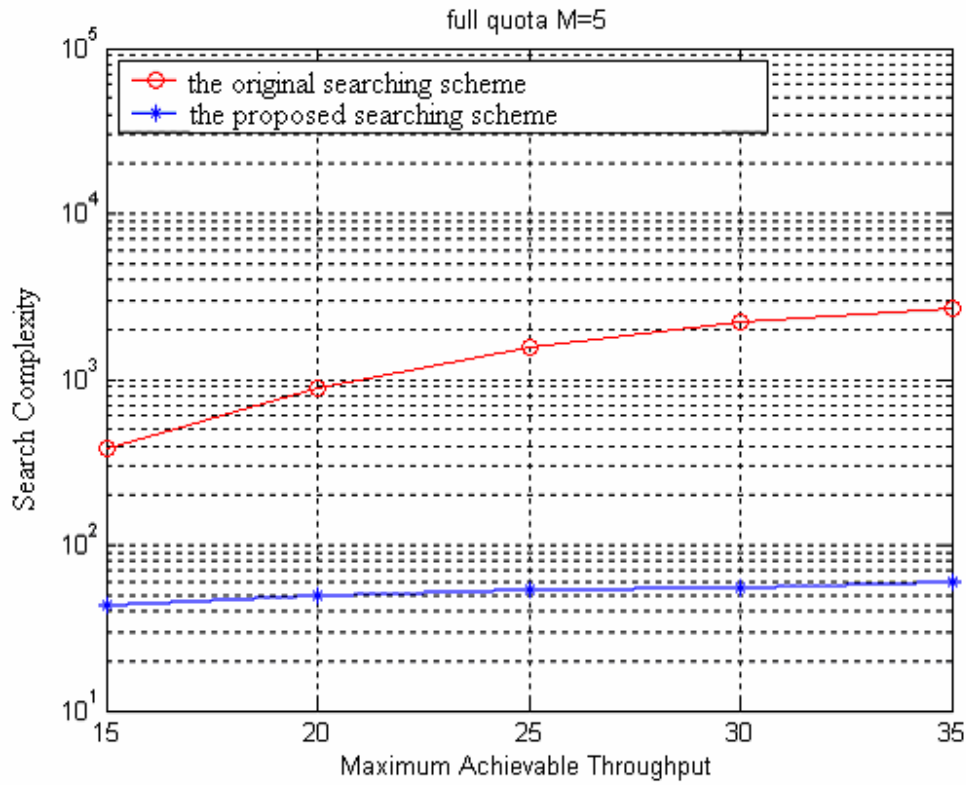
Figure 3.2   The Effects of Two Schemes Under Various $T\max$ (*M*=5)
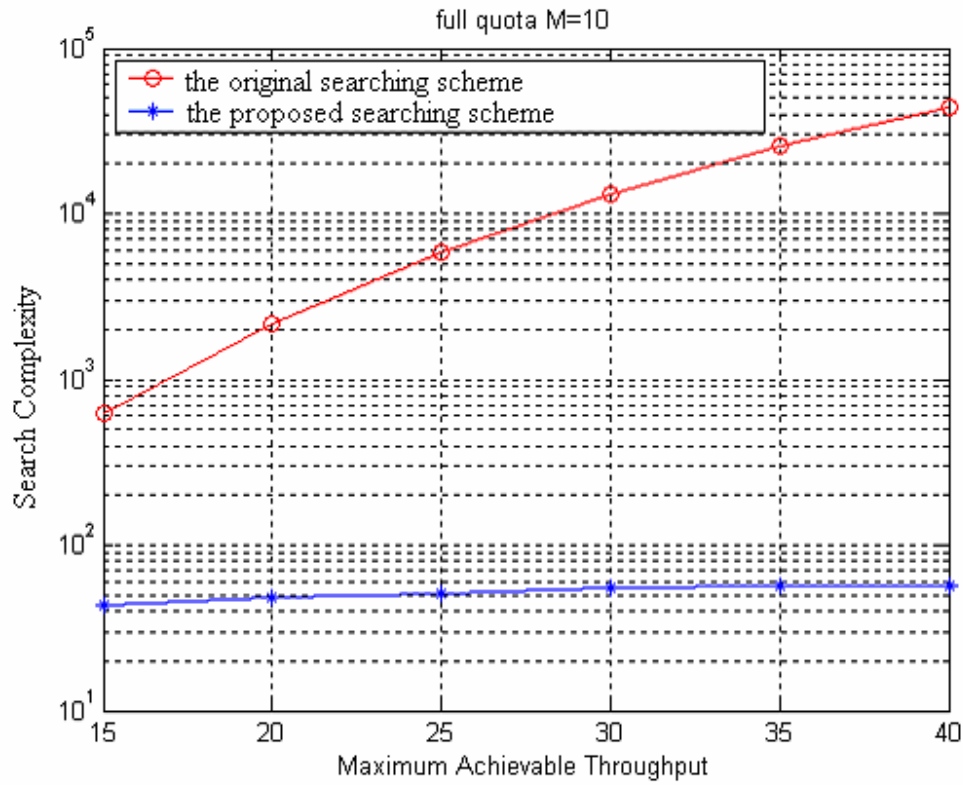
Figure 3.3   The Effects of the Two Schemes Under Various $T\max$ **(*M*=10)**
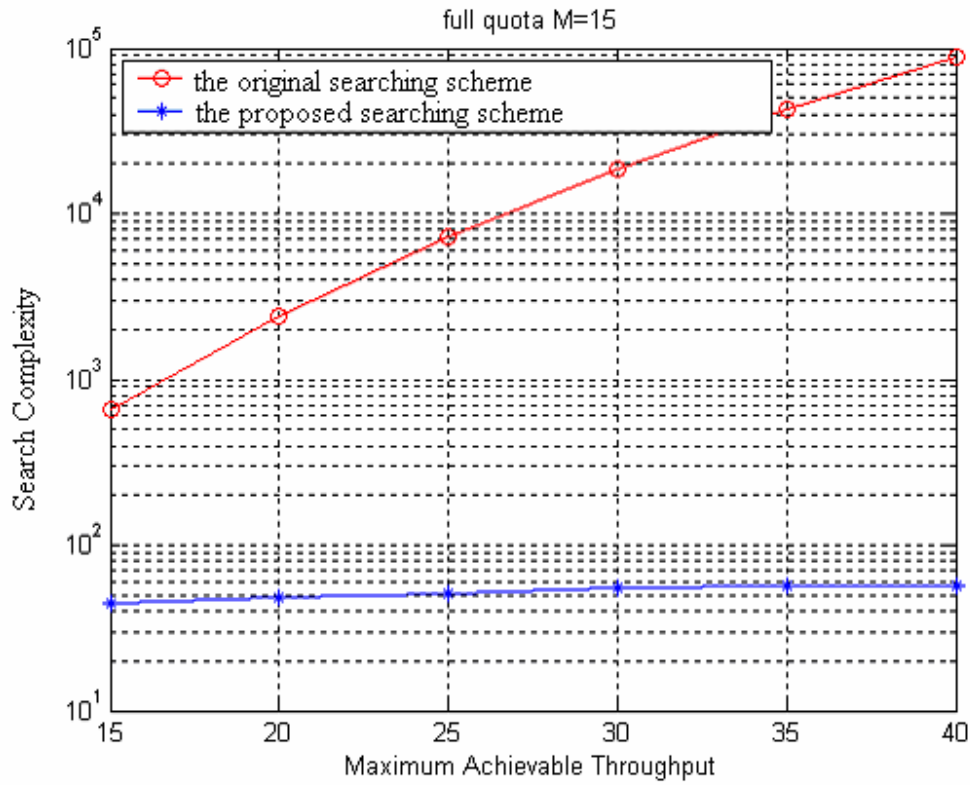
Figure 3.4   The Effects of Two Schemes Under Various $T\max$ (M =15)

Chapter 4 Conclusion

4.1 Summary of Thesis

The radio link for either a mobile portable or a vehicular unit involves transmission quality that varies with time. When the transmitter is provided with the channel state information, the transmission schemes can be adapted to it, allowing the channel to be used more efficiently. In general, combined rate and power control will dominate in next generation CDMA systems.

In Chapter 1, we start with introduction of the mobile radio channel. The features like mulitpath propagation associated with the radio wave make wireless communication very different with wired counterpart. To make the communication more efficient, several air interfaces have been proposed and put into commercial use. Among them, CDMA is deemed to be one of the most promising technologies with some advantages over its counterparts. We next come to introduce two key adaptation techniques used in CDMA systems, which are power control and rate control. Both aim to improve the system's capacity by adjusting the transmitter's power and rate according to the channel conditions.

In Chapter 2, in order to obtain a wireless channel model for further use in Chapter 3 a channel simulation model is provided based on Clarke's scattering model[4]. We focus on the design of Doppler filter which is an essential part of the simulator. Although we only generate the flat fading channel with Rayleigh distribution, it also can be used to form frequency selective fading channel by constructing two-ray channel model. To verify the

validity of the simulated outcome, we conduct first-order statistical analysis (distribution) and second-order statistical analysis (autocorrelation) to fading envelope and then we compare the evaluated curve with the theoretical curve. We find they agree very well.

Chapter 3 is the essential part of this dissertation in which an improved search scheme is proposed to reduce the search complexity in [19]. Several important conclusions are achieved as follows.

- We can narrow down the search range by applying proper boundary conditions therefore it enables us to analyze the case where full quota M is an unlimited integer. In the original scheme in [19], the value of M needs to be limited to within certain range. The reason for this is that if M goes to infinity, the size of the corresponding search table could increase to infinity almost exponentially. By narrowing down the search range, it avoids the need to search all achievable rate vectors outside the boundaries.

- When it comes to searching the optimal rate, it is possible to further reduce the searching complexity by adaptively adjusting the initial rate to the optimal one. That is mainly because we do not have to check every achievable rate vector within the boundary.

- The larger the value of full quota M is, the better the improvement we can receive with the proposed scheme. In the original scheme, the size of the search table rises almost exponentially as the value of M increases, while in the proposed scheme, the change in M only slightly affect the number of search steps.

4.2   Future Work

In this thesis, we proposed a more effective search scheme in maximization of uplink throughput in multicode CDMA systems. Once the channel fade is given, we can obtain the corresponding optimum rates transmitted by the users in order to maximize the instantaneous throughput. We have assumed perfect power and rate control as well as perfect channel estimation. However, in practice any system will have additional constraints arising out of the need to be fair to users in deep fades, other concerns like prolong battery life, or additional QoS requirements (delay constraints). Throughput for a practical system will also depend on the reliability and delay of the feedback channel, rate of adaptation and errors in the channel estimates.

It is interesting to apply the scheme to a more practical system where some of the above issues are assumed to be imperfect. For example, how to optimize the user's transmitted rate under a scenario where channel information is not available.

References

[1]   A. J. Viterbi, "CDMA: Principles of Spread Spectrum Communications," Addison Wesley, 1995.

[2]   D. Parsons, "The Mobile Radio Propagation Channel", Pentech Press, 1992.

[3]   T. Ottosson and A. Svensson, "Multirate Schemes in DS-CDMA Systems", IEEE Vehicular Technology Conference 1995, Vol.2, July 1995, pp.803-812.

[4]   R. H. Clarke, "A statistical theory of mobile radio reception", Bell Systems Technical Journal, Vol 47, November 1968, pp.241-244.

[5]   G. A. Arredondo, W. H. Chriss and E. H. Walker, "A Multi-path Fading Simulation for Mobile Radio", IEEE Transactions On Vehicular Technology, Vol VT-22, No 4, November 1973, pp241-244.

[6]   T. H. Wu and E. Geraniotis, "CDMA with multiple chip rates for multi-media communications," in Proc. Information Science and Systems, Princeton University, 1994, pp.992-997.

[7]   J. Zhu and G. Marubayashi, "Properties and application of parallel combinatory SS communication system," IEEE 2nd International Symposium on Spread Spectrum Techniques and Applications, Yokohama, Japan, Nov.29-Dec.2 1992, pp.227-230.

[8]   S. Ariyavisitakul, "Signal and interference statistics of a CDMA system with feedback power control –part II,"   IEEE Transactions on Communications, Vol. 42, No.2, February 1994, pp.597-605.

[9]   S. Ariyavisitakul and L. F. Chang, "Signal and interference statistics of a CDMA system with feedback power control," IEEE Transactions on Communications, Vol.41, No.11, November 1993, pp.1626-1634.

[10] S. J. Lee and W. J. Lee, "Capacities of Single-Code and Multicode DS-CDMA Systems Accommodating Muilticlass Services", IEEE Transactions on Vehicular Technology, Vol. 48, No. 2, March 1999, pp.376-384.

[11] K. M. Wasserman and S. J. Oh, "Dynamic Spreading Gain Control in Multi-Service CDMA Networks", IEEE Journal on Selected Areas in Communication. Vol.17, No.5, May 1999, pp.918-927.

[12] B. Hashem and E. Sousa, "A combined Power/Rate Control Scheme for Data Transmission Over a DS/CDMA system", IEEE Vehicular Technology Conference, Vol. 2, May 1998, pp.1096-1100.

[13] S. W. Kim and Y. H. Lee, "Combined Rate and Power Adaptation in DS/CDMA Communication over Nakagami Fading Channels" IEEE Transactions on Communications, Vol.48, No.1, January 2000, pp.162-168.

[14] H. D. Schotten, H. Elders-Boll and A. Busboom, "Multi-Code CDMA with Variable Sequence Sets". IEEE 6th International Conference on Universal Personal Communications, Vol. 2, 12-16 Oct 1997, pp.621-631.

[15] A. J. Goldsmith and S. G. Chua, "Variable Rate Variable power MQAM for fading channels", IEEE Transaction on Communications, Vol. 45, No. 10, October 1997, pp.1218-1230.

[16] X. Qiu and K. Chawla, "Throughput Performance of Adaptive Modulation in Cellular Systems", IEEE International Conference on Universal Personal Communications, Vol.2, 5-9 Oct. 1998, pp.945-950.

[17] S. W. Kim and A. Goldsmith, "Truncated power control in CDMA communications" IEEE Globle Telecommunications Conference, Vol. 3, Nov. 1997, pp.1488-1493.

[18] S. A. Jafar and A. Goldsmith, "Optimal Rate and Power Adaptation for Multirate CDMA", IEEE Vehicular Technology Conference, Vol. 3, 24-28 Sept. 2000, pp.994-1000.

[19] A. J. Syed and A. J. Goldsmith, "Adaptive Multicode CDMA for Uplink Throughput Maximization", available at http://wsl.stanford.edu/Publications/Syed/j1.ps.

[20] I. S. Gradshteyn, I. M. Ryzhik, "Table of Integrals, Series and Products", Academic Press, 1994.

[21] A. Baier, U. C. Feibig, W.Granzow, P. Teder, and J. Thielecke, "Design study for a CDMA-based third-generation mobile radio system", IEEE Journal on Selected Areas in Communications, Vol. 12, No.4, May 1994, pp.733-743.

[22] T. H. Wu and E. Geraniotis, "CDMA with Multiple Chip Rates for Multi-Media Communications". Proceedings of the 28th Annual Conference on Infomation Sciences, Alberta Canada, May 2000.

[23] S. H. Won, W. W. Kim and I. M. Jeong, "Performance Improvement of CDMA Power Control In Variable Fading Environments", IEEE Proceedings Southeastcon '97, 'Engineering New Century', Apr 1997, pp.241-243.

Appendix A   Source Code of Channel Fading Model

```
%++++++++++++++++++++++++++++++++++++++++++++++++++++++++++++++++++++++++%

% This program is designed to simulate the multipath wireless channel with a Rayleigh

% distribution. Both first order and second order statistics are performed to verify the

% validity of the simulated results by comparing them with the theoretical values.

%++++++++++++++++++++++++++++++++++++++++++++++++++++++++++++++++++++++++%


% define the necessary parameters for the system

   length=4096;                              % define the block length of Doppler filer

   filter_sample_num=41;                     % number of samples used to sample

   total_length=12288*10;                    % number of samples needed to be simulated

   STDf=1;

   v=100*1000/3600;                          % vehicular  velocity

   Fd=20;                                    % Doppler frequency

   sample_rate=Fd*length/filter_sample_num;              % sampling rate

   fd=Fd-.1;

   t=0:1/sample_rate:(total_length-1)*1/sample_rate;     % time vector

   t=t';

   Wc=2*pi*900000000;                        % carrier frequency

   k=2;                                      % number of fading channel

   space_di=1;                               % space diversity
```

```matlab
% Generate Doppler impulse response
%++++++++++++++++++++++++++++++++++++++++++++++++++++++++++++++++++++++++%
  x=-fd:fd/filter_sample_num:fd;
  y=(sqrt(1./sqrt(1-(x/Fd).^2)))';        % normalized doppler filter's frequency response


  % Hf denotes the sampled frequency response
  % Ht denotes the sampled Doppler filter's response


  Hf=zeros(length,1);
  Hf(1:filter_sample_num,1)=y(filter_sample_num+2:2*filter_sample_num+1,1);
  Hf(length-filter_sample_num+1:length,1)=y(1:filter_sample_num,1);
  Ht=real(ifft(Hf,length));


 %the following manipulations are needed to reorganise Doppler filter's impulse response


  Ht1=zeros(length+length/2,1);
  Ht1(1:length/2,1)=Ht(length/2+1:length,1);
  Ht1(length/2+1:length,1)=Ht(1:length/2,1);
  Ht=Ht1;                             %  Doppler filter's impulse response
  plot(1:length,Ht(1:length,1));
  Hf=fft(Ht);
```

```
Rt=zeros(total_length,k*space_di);          % denotes envelop r(t)

real_part=zeros(total_length,k*space_di);

imag_part=zeros(total_length,k*space_di);

% complex form of Rayleight fading

complex_AWGN=zeros(total_length, k*space_di);

for m=1:k*space_di

  % Generate the white Gaussian noise sequences

    w1=randn(total_length,1);

    w2=randn(total_length,1);

    Xt=zeros(total_length,1);

    Yt=zeros(total_length,1);


% Carry out the discrete convolution chunk by chunk
%++++++++++++++++++++++++++++++++++++++++++++++++++++++++++++++++++++
  for outrun=0:total_length/length*2-1

      chunk_length=length+length/2;   %convolution for upper branch

      chunk=zeros(chunk_length,1);

      chunk(1:length/2,1)=w1(outrun*length/2+1:(outrun+1)*length/2,1);

      f_domain1=fft(chunk).*Hf;

      t_domain1=ifft(f_domain1);

      chunk=zeros(chunk_length,1);    % convolution for lower branck

      chunk(1:length/2,1)=w2(outrun*length/2+1:(outrun+1)*length/2,1);

      f_domain2=fft(chunk).*Hf;
```

```
    t_domain2=real(ifft(f_domain2));

   %perform overlapping

  if outrun==total_length/length*2-1

  Xt(outrun*length/2+1:(outrun+1)*length/2,1)=...

    Xt(outrun*length/2+1:(outrun+1)*length/2,1)+t_domain1(1:length/2,1);

  Yt(outrun*length/2+1:(outrun+1)*length/2,1)=...

    Yt(outrun*length/2+1:(outrun+1)*length/2,1)+t_domain2(1:length/2,1);

  else

    if outrun==total_length/length*2-2

      Xt(outrun*length/2+1:(outrun+2)*length/2,1)=...

        Xt(outrun*length/2+1:(outrun+2)*length/2,1)+t_domain1(1:length,1);

      Yt(outrun*length/2+1:(outrun+2)*length/2,1)=...

        Yt(outrun*length/2+1:(outrun+2)*length/2,1)+t_domain2(1:length,1);

    else

      Xt(outrun*length/2+1:(outrun+3)*length/2,1)=...

        Xt(outrun*length/2+1:(outrun+3)*length/2,1)+t_domain1(:,1);

      Yt(outrun*length/2+1:(outrun+3)*length/2,1)=...

        Yt(outrun*length/2+1:(outrun+3)*length/2,1)+t_domain2(:,1);

    end

  end

end


% combine the x(t) and y(t) to obtain normalize envelope r(t)
```

```
    i=1:total_length;

    Xt=1/sample_rate*real(Xt);

    Yt=1/sample_rate*real(Yt);

    Rt(1:total_length,m)=sqrt((Xt).^2+(Yt).^2);

    mean_value=mean(Rt(length/2+1:total_length,m));

    Rt(1:total_length-length/2,m)=Rt(length/2+1:total_length,m)/mean_value;


    real_part(1:total_length-length/2,m)=real(Xt(length/2+1:total_length))/mean_value;

    imag_part(1:total_length-length/2,m)=real(Yt(length/2+1:total_length))/mean_value;
end


%++++++++++++++++++++++++++++++++++++++++++++++++++++++++++++++++++++++++%

%testify the simulation result

% 1. obtain  typical Rayleigh faded envelope

% 2. obtain the pdf of the envelope and compare with theoretical pdf

% 3. obtain the autocorrelation of the envelope and compare with the theoretical values

%++++++++++++++++++++++++++++++++++++++++++++++++++++++++++++++++++++++++%


complex_AWGN=real_part+j*imag_part;

envelope=20*log10(Rt(1:total_length-length/2,1));

i=1:2000;
```

%1. Plot the faded envelope r(t)

```
figure(2);

plot(i*1/sample_rate,envelope(length+i));

title('Rayleigh fading envelope');

xlabel(' Time (sec) ');

ylabel(' Envelope Level (dB)');

axis([0, 2000*1/sample_rate, -40, 20]);
```

%2. plot the distribution of the faded envelop

```
figure(3);

counter=zeros(200,1);

for i=1+length:total_length-length

    j=0;

    upper_bound=4;

    lower_bound=0;

    upper=upper_bound;

    lower=lower_bound;

    if  Rt(i)<lower_bound


    elseif Rt(i)<upper_bound

        while Rt(i)>lower
```

```
                lower=lower+(upper_bound-lower_bound)/200;

                j=j+1;

            end

            counter(j)=counter(j)+1;

        else


        end

    end

end

x=1:200;

Rt1=Rt(length+1:total_length);


signal_var=mean(Rt(length+1:total_length-length,1))/1.2533;

sum(counter)


plot(x*(upper_bound-lower_bound)/200,...

    counter(x)/((total_length-2*length)*(upper_bound-lower_bound)/200),'k')

hold on

x=lower_bound:(upper_bound-lower_bound)/200:upper_bound;

plot(x, x./signal_var^2.*exp(-x.^2/(2*signal_var^2)),':');

ylabel(' PDF of Rayleigh faded envelope ');

legend('\it simulated','\it theoretical');

xlabel(' Amplitude of the envelope ');

hold off
```

```matlab
  %3.second order statistics

 %compute and plot the autocorrelation of r(t)

 figure(4);

 T=1/sample_rate*total_length;

 delay=4096;

 autocorrelation=zeros(delay,1);

 for i=1:delay

   autocorrelation(i)=sum(Xt(i+length:total_length,1).*...

     Xt(1+length:total_length-i+1,1))/(2*(total_length-length));

 end

 i=1:1000;

 plot(i,autocorrelation(i)/autocorrelation(1));

 hold on

 theo_auto=.5*std(Xt)^2*besselj(0,2*pi*(Fd-.1)*(i-1)*1/sample_rate);

 plot(i,theo_auto(i)/theo_auto(1),'r:');

 legend('\it simulated','\it theoretical');

 title('Autocorrelation : second-order statistics');

 xlabel(' delay \tau normalized to sample period');

 ylabel(' the amplitude is normalized to 1');

 hold off

 x=1:total_length;

%end of the program
```

Appendix B Source Code of The Improved Scheme

B.1   In Case of M as an Unlimited Integer

```
%**********************************************************************%
% This simulation model is designed to obtain the average searching steps for the newly
% improved search scheme in case that rate full quota M is unlimited. For more details,
% Please refer to the corresponding content presented in Chapter 3.
%**********************************************************************%


%  define system's parameters

N=63;                        % spreading gain

Mmax1=21;                    % number of bit rates 0 ,  1, 2 , 4

Max=22;

K=10;                        % number of user

BER=0.0011;                  % required bit error rate

Emax_No=12;                  %   in db

Smax=0.2;                    % the maximum transmitted power=0.2w

Tb=1/10000;                  % symbol rate

No=Smax*Tb/(10^(Emax_No/10));      % AWGN spectral density

SNRo=(erfcinv(2*BER))^2;            % required SNR corresponding to the BER

D=3*N/(2*SNRo);              %  D and C are the same notation as that in the algorithm
```

```
C=3*N*No/(2*Tb);

load fading;                         %  channel flat fading  gain obtainable in Chapter 2

Ni=zeros(length(fading(1,:)),K);

Ni1=zeros(length(fading(1,:)),K);

max_achieve=0;

num_step=zeros(length(fading(1,:)),1);



%********************************************************************%

% start to search the optimal rate vector given the channel information according to the

%algorithm presented in Chapter 3.

%********************************************************************%

for h=1:10000;

    fading(1:K,h)=flipud(sort(abs(fading(1:K,h))));

    g=abs(fading(1:K,h)).^2;

    for  n=K:-1:2;

        Ni(2,:)=zeros(1,K);

        Ni(1,1:n)=D*g(1:n)'*Smax/C*(1-sum(g(1:n))*Smax/C/(sum(g(1:n))*Smax/C+1))

./(1-g(1:n)'*Smax/C*(1-sum(g(1:n))*Smax/C/(sum(g(1:n))*Smax/C+1)));

        Ni(2,1:n-1)=floor(Ni(1,1:n-1));

        Ni(2,n)=ceil(Ni(1,n));

        num_step(h)=num_step(h)+1;

        y=sum(Ni(2,1:n)./(Ni(2,1:n)+D));

        fading_limit=C/Smax*(Ni(2,1:n)./(Ni(2,1:n)+D))*1/(1-y);
```

```
if min(abs(fading(1:n,h)').^2>=fading_limit)==0

    Ni(2,n)=Ni(2,n)-1;

     if Ni(2,n)==0

         continue;

      end

 end

 max_tail=Ni(2,n);

 for j=max_tail:-1:max(max_tail-n,1)

     Ni(2,n)=j;

     Ni(2,1:n-1)=floor(Ni(1,1:n-1));

     for i=1:n+1

        [a,b]=min((Ni(2,1:n)+1-Ni(1,1:n))./(Ni(1,1:n)));

        num_step(h)=num_step(h)+1;

        y=sum(Ni(2,1:n)./(Ni(2,1:n)+D));

        y2(1:n-1)=y-Ni(2,1:n-1)./(Ni(2,1:n-1)+D)+(Ni(2,1:n-1)+1)./(Ni(2,1:n-
1)+1+D)-Ni(2,n)./(Ni(2,n)+D)+(Ni(2,n)-1)/(Ni(2,n)-1+D);

        y1=sum(Ni(1,1:n)./(Ni(1,1:n)+D));

        [a,b]=max((1-(Ni(2,1:n-1)+1)./(Ni(2,1:n-1)+1+D)./(1-y2(1:n-1))./
(Ni(1,1:n-1)./(Ni(1,1:n-1)+D)/(1-y1))));%.*(Ni(2,1:n)+1));

        if a<0

            break;

         end

        Ni(2,b)=Ni(2,b)+1;
```

```
y=sum(Ni(2,1:n)./(Ni(2,1:n)+D));

fading_limit=C/Smax*(Ni(2,1:n)./(Ni(2,1:n)+D))*1/(1-y);

if min(abs(fading(1:n,h)').^2>=fading_limit)==0

    Ni(2,b)=Ni(2,b)-1;

     break;

   end

 end

if sum(Ni(2,:)')>=sum(Ni1(h,:)')

    Ni1(h,:)=Ni(2,:);

    if sum(Ni1(h,:))>max_achieve

       max_achieve=sum(Ni1(h,:));

     end

  end

 end

end

Ni(2,:)=[floor(D*abs(fading(1,h))^2*Smax/C) zeros(1,K-1)];

num_step(h)=num_step(h)+1;

if sum(Ni(2,:)')>=sum(Ni1(h,:)')

   Ni1(h,:)=Ni(2,:);

   if sum(Ni1(h,:))>max_achieve

      max_achieve=sum(Ni1(h,:));

    end

end
```

```
end

max_achieve

mean(num_step(1:10000))                    % calculate average number of  search steps
```

B.2   In Case of *M* as a Limited Integer

```
%*****************************************************************%
% This simulation model is designed to obtain the average searching steps  for the newly
% improved  search scheme  in case that rate full quota M is limited. For more details,
%Please refer to Chapter 3.
%*****************************************************************%
% define the  basic parameters and variables for the systems as following
N=63;                        % spreading gain
Mmax1=21;
Mmax=10;
Max=22;
K=10;                        % number of user
BER=0.0011;                   % required bit error rate
Emax_No=12;                   % Emax=Smax*Tb   in db
Smax=0.2;                     % the maximum transmitted power=0.2w
Tb=1/10000;                   % symbol rate
No=Smax*Tb/(10^(Emax_No/10));       % AWGN spectral density
SNRo=(erfcinv(2*BER))^2;            % required SNR corresponding to the BER
p=0;                               % used to store the number of users  at full M quotas
D=3*N/(2*SNRo);
C=3*N*No/(2*Tb);
```

```
load fading;                            % generated from the flat fading simulation

Ni=zeros(length(fading(1,:)),K);

Ni1=zeros(length(fading(1,:)),K);

max_achieve=0;                          % used to count maximal throughput

num_step=zeros(length(fading(1,:)),1); % used to count number of searching steps



%*****************************************************************%

 % start to search the optimum rate vector given the channel gain vector

%*****************************************************************%



 for h1=1:10000;                        % number of vectors  need to be simulated

    % sort channel gain in decreasing order

     fading(1:K,h1)=flipud(sort(abs(fading(1:K,h1))));

     g=abs(fading(:,h1)).^2;            % channel power vector

     for  h=K:-1:2;                     % nh range from

         Ni(2,:)=zeros(1,K);

         Ni(1,1:h)=D*g(1:h)'*Smax/C*(1-sum(g(1:h))*Smax/ C/(sum(g(1:h))*Smax…

/C+1)) ./(1-g(1:h)'*Smax/C*(1-sum(g(1:h))*Smax/C/(sum(g(1:h))*Smax/C+1)));

         p=0;

         for i=1:h                      % calculate  the value of p

            if Ni(1,i)>=Mmax

            p=p+1;

            end
```

```matlab
    end

    for j=1:Mmax

        Ni(2,1:h-1)=floor(Ni(1,1:h-1));

        Ni(2,h)=j;

        for i=1:h-1

            Ni(2,i)=min(Mmax,Ni(2,i));

        end

        num_step(h1)=num_step(h1)+1;

        y=sum(Ni(2,1:h)./(Ni(2,1:h)+D));

         %lower baund of fading given the rate vector;

         fading_limit=C/Smax*(Ni(2,1:h)./(Ni(2,1:h)+D))*1/(1-y);

         if min(abs(fading(1:h,h1)').^2>=fading_limit)==0

            Ni(2,h)=Ni(2,h)-1;

            if Ni(2,h)==0

                continue;

            end

         end

        %max_tail=Ni(2,n);

         for i=1:Max

             num_step(h1)=num_step(h1)+1;

             y=sum(Ni(2,1:h)./(Ni(2,1:h)+D));

             y2(1:h-1)=y-Ni(2,1:h-1)./(Ni(2,1:h-1)+D)+

(Ni(2,1:h-1)+1)./(Ni(2,1:h-1)+1+D)-Ni(2,h)./(Ni(2,h)+D)+(Ni(2,h)-1)/(Ni(2,h)-1+D);
```

```
            y1=sum(Ni(1,1:h)./(Ni(1,1:h)+D));

            [a,b]=max((1-(Ni(2,p+1:h-1)+1)./(Ni(2,p+1:h-1)+1+D)./(1-y2(p+1:h-

1))./(Ni(1,p+1:h-1)./(Ni(1,p+1:h-1)+D)/(1-y1))));%.*(Ni(2,1:n)+1));

            if a<0

               break;

             end

            Ni(2,b)=Ni(2,b)+1;

            if Ni(2,b)==Mmax

               p=p+1;

            end

            y=sum(Ni(2,1:h)./(Ni(2,1:h)+D));

            fading_limit=C/Smax*(Ni(2,1:h)./(Ni(2,1:h)+D))*1/(1-y);

            if min(abs(fading(1:h,h1)').^2>=fading_limit)==0

               Ni(2,b)=Ni(2,b)-1;

               break;

            end

         end

         if sum(Ni(2,:)')>=sum(Ni1(h1,:)')

            Ni1(h1,:)=Ni(2,:);

            if sum(Ni1(h1,:))>max_achieve

               max_achieve=sum(Ni1(h1,:));

            end

         end
```

```
        end

    end

    Ni(2,:)=[min(Mmax,floor(D*abs(fading(1,h1))^2*Smax/C)) zeros(1,K-1)];

    num_step(h1)=num_step(h1)+1;

    if sum(Ni(2,:)')>=sum(Ni1(h1,:)')

        Ni1(h1,:)=Ni(2,:);

        if sum(Ni1(h1,:))>max_achieve

            max_achieve=sum(Ni1(h1,:));

        end

    end

end

max_achieve

mean(num_step(1:100000))                 % calculate  average searching steps
```